



## Partitioning soil organic carbon into its centennially stable and active fractions with statistical models based on Rock-Eval® thermal analysis (PARTY<sub>SOC</sub>v2.0 and PARTY<sub>SOC</sub>v2.0<sub>EU</sub>)

5 Lauric Cécillon<sup>1,2</sup>, François Baudin<sup>3</sup>, Claire Chenu<sup>4</sup>, Bent T. Christensen<sup>5</sup>, Uwe Franko<sup>6</sup>, Sabine Houot<sup>4</sup>,  
Eva Kanari<sup>2,3</sup>, Thomas Kätterer<sup>7</sup>, Ines Merbach<sup>8</sup>, Folkert van Oort<sup>4</sup>, Christopher Poeplau<sup>9</sup>, Juan Carlos  
Quezada<sup>10,11,12</sup>, Florence Savignac<sup>3</sup>, Laure N. Soucémariandin<sup>13</sup>, Pierre Barré<sup>2</sup>

<sup>1</sup>Laboratoire ECODIV, Univ. Normandie, UNIROUEN, INRAE, FR Scale CNRS 3730, Rouen, 76000, France

10 <sup>2</sup>Laboratoire de Géologie, CNRS, École normale supérieure, PSL University, IPSL, Paris, France

<sup>3</sup>Institut des Sciences de la Terre de Paris, Sorbonne Université, CNRS, Paris, 75005, France

<sup>4</sup>UMR 1402 ECOSYS, INRAE, AgroParisTech, Univ. Paris Saclay, Thiverval-Grignon, 78850, France

<sup>5</sup>Department of Agroecology, Aarhus University, AUFOULUM, 8830 Tjele, Denmark

<sup>6</sup>Department of soil system science, Helmholtz Centre for Environmental Research, UFZ, 06120 Halle Germany

15 <sup>7</sup>Department of Ecology, Swedish University of Agricultural Sciences, 75007 Uppsala, Sweden

<sup>8</sup>Department Community Ecology, Helmholtz Centre for Environmental Research, UFZ, 06246 Bad Lauchstädt, Germany

<sup>9</sup>Thünen Institute of Climate-Smart Agriculture, 38116 Braunschweig, Germany

<sup>10</sup>Laboratory of Ecological Systems ECOS and Laboratory of Plant Ecology Research PERL, School of Architecture, Civil and Environmental Engineering ENAC, École Polytechnique Fédérale de Lausanne EPFL, 1015 Lausanne, Switzerland

20 <sup>11</sup>Swiss Federal Institute for Forest, Snow and Landscape Research WSL, 1015 Lausanne, Switzerland

<sup>12</sup>Ecosystem Management, Institute of Terrestrial Ecosystems, Department of Environmental Systems Science, ETHZ, 8092 Zürich, Switzerland

<sup>13</sup>ACTA – les instituts techniques agricoles, 75595 Paris, France

25 Correspondence to: Lauric Cécillon ([lauric.cecillon@inrae.fr](mailto:lauric.cecillon@inrae.fr))



## Abstract

Partitioning soil organic carbon (SOC) into two kinetically different fractions that are centennially stable or active is key information for an improved monitoring of soil health and for a more accurate modelling of the carbon cycle. However, all 30 existing SOC fractionation methods isolate SOC fractions that are mixtures of centennially stable and active SOC. If the stable SOC fraction cannot be isolated, it has specific chemical and thermal characteristics that are quickly (*ca.* 1 h per sample) measureable using Rock-Eval® thermal analysis. An alternative would thus be to (1) train a machine-learning model on the Rock-Eval® thermal analysis data of soil samples from long-term experiments where the size of the centennially 35 stable and active SOC fractions can be estimated, and (2) apply this model on the Rock-Eval® data of unknown soils, to partition SOC into its centennially stable and active fractions. Here, we significantly extend the validity range of the machine-learning model published by Cécillon et al. [Biogeosciences, 15, 2835–2849, 2018, <https://doi.org/10.5194/bg-15-2835-2018>], and built upon this strategy. The second version of this statistical model, which we propose to name  $\text{PARTY}_{\text{SOC}}$ , uses six European long-term agricultural sites including a bare fallow treatment and one South American vegetation change ( $\text{C}_4$  to  $\text{C}_3$  plants) site as reference sites. The European version of the model ( $\text{PARTY}_{\text{SOCv2.0}_{\text{EU}}}$ ) predicts the proportion of the 40 centennially stable SOC fraction with a conservative root-mean-square error of 0.15 (relative root-mean-square error of 0.27) in a wide range of agricultural topsoils from Northwestern Europe. We plan future expansions of the  $\text{PARTY}_{\text{SOC}}$  global model using additional reference soils developed under diverse pedoclimates and ecosystems, and we already recommend the application of  $\text{PARTY}_{\text{SOCv2.0}_{\text{EU}}}$  in European agricultural topsoils to provide accurate information on SOC kinetic pools partitioning that may improve the simulations of simple models of SOC dynamics.

45



## 1 Introduction

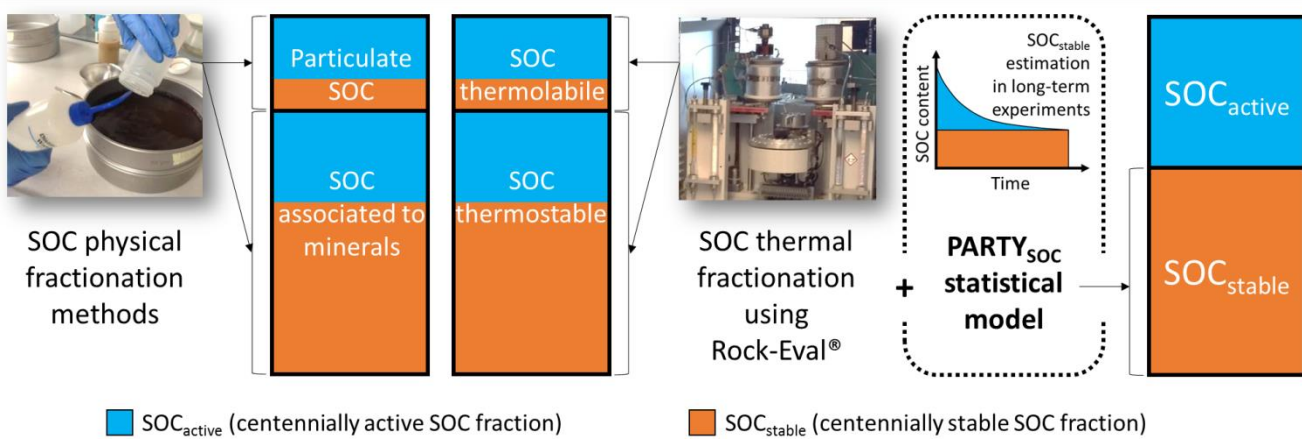
Soil organic carbon (SOC) is identified as a key element contributing to soil functions such as primary productivity, water purification and regulation, carbon sequestration and climate regulation, habitat for biodiversity and recycling of nutrients (Keesstra et al., 2016; Koch et al., 2013; Schulte et al., 2014; Wiesmeier et al., 2019). While the magnitude and the historical dimension of the decrease in SOC at the global level are progressively being unveiled (IPBES, 2018; Sanderman et al., 2017; Stoorvogel et al., 2017), SOC stocks' preservation and even increase is a major challenge for human societies in the 21<sup>st</sup> century (Amundson et al., 2015). With widespread beneficial effects on soil functioning at the local level (Pellerin et al., 2019), increasing the size of the global SOC reservoir contributes directly to the Sustainable Development Goal related to life on land (<https://www.globalgoals.org/15-life-on-land>). It is also one of the few land management-based intervention options that has a broad and positive impact on food security and climate change mitigation and adaptation, two other Sustainable Development Goals set by the United Nations (IPCC, 2019; Lal, 2004).

There is experimental evidence showing that in all soils, SOC is made of carbon atoms with highly contrasting residence times, ranging from hours to millennia (Balesdent et al., 1987; Trumbore et al., 1989). This continuum in SOC persistence is often simplified by considering SOC as a mixture formed of several fractions, also called kinetic pools by modelers (Hénin and Dupuis, 1945; Jenkinson, 1990; Nikiforoff, 1936). The most drastic conceptual simplification of SOC persistence considers only two pools: (1) one made of young SOC with a short turnover rate (typically three decades on average; the active or labile SOC pool) and (2) one made of older SOC that persists much longer in the soil (more than a century; the stable, passive or persistent SOC pool). This dualistic representation of SOC persistence was considered as "*a necessary simplification, but certainly not a utopian one*" four decades ago (Balesdent and Guillet, 1982) and is still considered as meaningful (e.g., Lavallee et al., 2020). The active and stable soil organic matter pools contribute differently to the various soil functions (Hsieh, 1992). The active organic matter pool efficiently fuels soil biological activity (with carbon, nutrients and energy) and plant growth (with nutrients) through its rapid decay, and it sustains soil structure development (Abiven et al., 2009; Janzen, 2006). Conversely, the potential contribution of a soil to climate regulation would be most dependent on its stable organic matter pool size (He et al., 2016; Shi et al., 2020).

A myriad of methods has been developed and tested to partition SOC into active and stable fractions, that would match kinetic pools for the assessment of SOC dynamics and related soil functions, since the second half of the 20<sup>th</sup> century (Balesdent, 1996; Hénin and Turc, 1949; Monnier et al., 1962; Poeplau et al., 2018). Some of these methods based on chemical or physical (size, density or thermal) fractionation schemes can separate SOC fractions with, on average, different turnover rates (Balesdent, 1996; Plante et al., 2013; Poeplau et al., 2018; Trumbore et al., 1989). Of these methods, only a few are reasonably reproducible and easy to implement such as the ones based on rapid thermal analysis and chemical extractions (Gregorich et al., 2015; Poeplau et al., 2013, 2018; Soucémarianadin et al., 2018a). Other methods, such as size



and density SOC fractionation, need to be inferred from statistical models or infrared spectroscopy to be implemented on 80 large soil sample sets (Baldock et al., 2013; Cotrufo et al., 2019; Jaconi et al., 2019; Viscarra Rossel et al., 2019; Viscarra Rossel and Hicks, 2015; Vos et al., 2018; Zimmermann et al., 2007b). However, all SOC fractionation methods fail to achieve a proper separation of stable from active SOC, and the isolated SOC fractions are thus mixtures of centennially stable and active SOC (Fig. 1; Balesdent, 1996; Hsieh, 1992; von Lützow et al., 2007; Sanderman and Grandy, 2020). This limitation is common to all existing SOC fractionation methods and compromises the results of any work using them directly 85 to quantify soil functions specifically related to SOC fractions or to parameterize SOC partitioning in multi-compartmental models of SOC dynamics (Luo et al., 2016). Simulations of SOC stocks changes by multi-compartmental models are very sensitive to the initial proportion of the centennially stable SOC fraction, underlining the importance of its accurate estimation (Clivot et al., 2019; Falloon and Smith, 2000; Jenkinson et al., 1991; Taghizadeh-Toosi et al., 2020).



90

**Figure 1: Conceptual representation of soil organic carbon fractionation methods vs. the  $\text{PARTY}_{\text{SOC}}$  approach to quantify the size of the centennially stable and active soil organic carbon fractions.** All existing soil organic carbon fractionation methods isolate fractions that are mixtures of centennially stable and active soil organic carbon.  $\text{PARTY}_{\text{SOC}}$  is a machine-learning model trained on the Rock-Eval® thermal analysis data of soil samples from long-term experiments where 95 the size of the centennially stable SOC fraction can be estimated. When applied on the Rock-Eval® data of unknown topsoils,  $\text{PARTY}_{\text{SOC}}$  partitions soil organic carbon into its active and stable fractions (*i.e.*, without isolating soil organic carbon fractions from each other). Abbreviation: SOC, soil organic carbon. Credits for photos: SOC physical fractionation methods, Mathilde Bryant; SOC thermal fractionation using Rock-Eval®, Lauric Cécillon.

100 If the stable SOC fraction cannot be isolated, it has specific chemical and thermal characteristics: stable SOC is depleted in hydrogen and thermally stable (Barré et al., 2016; Gregorich et al., 2015). These characteristics are quickly (*ca.* 1 h per sample) measurable using Rock-Eval® thermal analysis, and they could be of use to identify the quantitative contribution



of stable SOC to total SOC. An alternative to the elusive proper separation of stable and active SOC pools could thus be to directly predict their sizes by training a machine-learning model based on Rock-Eval® data to estimate the size of the stable 105 and active SOC fractions, without isolating them from each other (Fig. 1). This statistical model would need a learning set of soil samples for which SOC partitioning into its active and stable pools can be fairly estimated. Such soil samples are available in long-term (*i.e.*, at least longer than three decades) bare fallow experiments (LTBF; soils kept free of vegetation and thus with negligible SOC inputs), or long-term vegetation change ( $C_3$  plants to  $C_4$  plants or *vice versa*) experiments, as described by Balesdent et al. (1987, 2018), Barré et al. (2010), Cerri et al. (1985) or Rühlmann (1999). Cécillon et al. (2018) 110 used this strategy, developing a machine-learning random forests regression model on topsoil samples obtained from the archives of four European long-term agricultural sites including an LTBF treatment. This statistical model, which we propose to name  $\text{PARTY}_{\text{SOC}}$ , related thermal analysis parameters of topsoils measured with Rock-Eval® to their estimated proportion of the centennial stable SOC fraction (Fig. 1). This previous work positioned  $\text{PARTY}_{\text{SOC}}$  as the first operational method quantifying the centennial stable and active SOC fractions in agricultural topsoils from Northwestern Europe. 115 However, the ability of this machine-learning model to fairly partition the centennial stable and the active SOC fractions of soil samples from new sites in and outside Northwestern Europe is largely unknown because its learning sample set is (1) rather limited, with a low number of reference sites and (2) based on centennial stable SOC contents that are exclusively inferred from plant-free LTBF treatments.

120 In this study, we aimed to improve the accuracy and the genericity of the  $\text{PARTY}_{\text{SOC}}$  statistical model partitioning SOC into its centennial stable and active fractions developed by Cécillon et al. (2018). (1) We increased the range of soil types, soil texture classes, climates and types of long-term experiments, through the addition to the learning sample set of topsoils from three new reference sites (two additional European long-term agricultural sites with an LTBF treatment and one South-American long-term vegetation change site). (2) We integrated new predictor variables derived from Rock-Eval® thermal 125 analysis. (3) In this second version of the model, we also changed the following series of technical details. We added a new criterion based on observed SOC content to estimate of the size of the centennial stable SOC fraction at reference sites, to reduce the risk of overestimating this site-specific parameter. We calculated the proportion of the centennial stable SOC fraction differently in reference topsoil samples, using SOC content estimated by Rock-Eval® rather than by dry combustion. We changed some criteria regarding the selection of reference topsoils in the learning set of the model: we 130 removed samples from agronomical treatments with compost or manure amendments, and preference was given to samples with good organic carbon yield of their Rock-Eval® thermal analysis. We better balanced the contribution of each reference site to  $\text{PARTY}_{\text{SOCv2.0}}$ . (4) We also aimed to build a regional version of the statistical model restricted to the references sites available in Europe (named  $\text{PARTY}_{\text{SOCv2.0}_{\text{EU}}}$ ). (5) Finally, we carefully evaluated the performance of the statistical models on unknown reference sites, and we further investigated the sensitivity of model performance to the reference sites included 135 in the learning set. For clarity, the main changes between the first version of  $\text{PARTY}_{\text{SOC}}$  (Cécillon et al., 2018) and this second version of the model are summarized in supplementary Table S1.



## 2 Methods

### 2.1 Reference sites and estimation of the centennially stable SOC fraction content at each site

This second version of PARTY<sub>SOC</sub> uses seven long-term study sites as reference sites (*i.e.*, sites where the size of the 140 centennially stable SOC fraction can be estimated). The main characteristics of these seven reference sites and their respective soil type and basic topsoil properties are presented in supplementary Table S2, and more thoroughly in the references cited below. Six reference sites of PARTY<sub>SOCv2.0</sub> are long-term agricultural experiments located in Northwestern Europe that include at least one LTBF treatment. (1) The long-term experiment on animal manure and mineral fertilizers (B3- and B4-fields) and its adjacent LTBF experiment started in 1956 and terminated in 1985, at the Lermarken site of 145 Askov in Denmark (Christensen et al., 2019; Christensen and Johnston, 1997). (2) The static fertilization experiment (V120) started in 1902 and the fallow experiment (V505a) started in 1988 at Bad Lauchstädt in Germany (Franko and Merbach, 2017; Körschens et al., 1998; Ludwig et al., 2007). (3) The “36 parcelles” experiment, started in 1959 at Grignon in France (Cardinael et al., 2015; Houot et al., 1989). (4) The “42 parcelles” experiment, started in 1928 at Versailles in France (van Oort et al., 2018). (5) The Highfield bare fallow experiment, started in 1959 at Rothamsted in England (Johnston et al., 150 2009). (6) The Ultuna continuous soil organic matter field experiment, started in 1956 in Sweden (Kätterer et al., 2011). These six reference sites are used in the European version of the statistical model, PARTY<sub>SOCv2.0<sub>EU</sub></sub>. One additional long-term vegetation change site completes the reference sites list of the PARTY<sub>SOCv2.0</sub> global statistical model. This site is a 56-year chronosequence of oil palm plantations (with C<sub>3</sub> plants) established on former pastures (with C<sub>4</sub> plants), located in South-America (La Cabaña in Colombia), and sampled as a space-for-time substitution (Quezada et al., 2019).

155

For each reference site, data on total SOC content in topsoil (0–10 cm to 0–30 cm depending on the site; supplementary Table S2) were obtained from previously published studies (Barré et al., 2010; Cécillon et al., 2018; Franko and Merbach, 2017; Körschens et al., 1998; Quezada et al., 2019). Total SOC content was measured by dry combustion with an elemental 160 analyzer (SOC<sub>EA</sub>, g C kg<sup>-1</sup>) according to ISO 10694 (1995), after the removal of soil carbonates using an HCl treatment for the topsoils of Grignon. For the site of La Cabaña, data on <sup>13</sup>C content (measured using an isotope-ratio mass spectrometer coupled to the elemental analyzer, the results being expressed in δ<sup>13</sup>C abundance ratio (‰ relative to the international standard)) were obtained from Quezada et al. (2019), and the relative contributions of new (C<sub>3</sub>-plant derived) and old (C<sub>4</sub>-plant derived) carbon to total SOC in topsoils (0–10 cm) were calculated using the Equation 3 of the paper published by Balesdent and Mariotti (1996), as done in Quezada et al. (2019).

165

Based on these published data, the content of the centennially stable SOC fraction (g C kg<sup>-1</sup>) at each reference site was estimated by modelling the decline of total SOC present at the onset of the experiment with time (sites with an LTBF treatment; as SOC inputs are negligible in bare fallow systems) or by modelling the decline of C<sub>4</sub>-plant derived SOC present at the time of vegetation change with time (La Cabaña site; as SOC inputs from C<sub>4</sub> plants are negligible after pasture



170 conversion to oil palm plantation). For the seven reference sites, the decline in total SOC or C<sub>4</sub>-plant derived SOC over time had a similar shape, as shown in Barré et al. (2010), Cécillon et al. (2018), Franko and Merbach (2017) and Quezada et al. (2019) and could be modelled using a first-order exponential decay with a constant term following Eq. (1):

$$\gamma(t) = ae^{-bt} + c, \quad (1)$$

175 where  $\gamma(t)$  (g C kg<sup>-1</sup>) is the total (sites with an LTBF treatment) or C<sub>4</sub>-plant derived (La Cabaña site) SOC content at time  $t$ ,  $t$  (year) is the time under bare fallow (sites with an LTBF treatment) or since pasture conversion to oil palm plantation (La Cabaña site), and  $a$ ,  $b$  and  $c$  are fitting parameters. Parameter  $a$  (g C kg<sup>-1</sup>) corresponds to the content of the active SOC fraction and  $b$  (yr<sup>-1</sup>) is the characteristic decay rate. The parameter  $c$  (g C kg<sup>-1</sup>) represents the content of theoretically inert SOC. Following Barré et al. (2010), Cécillon et al. (2018) and Franko and Merbach (2017), we considered this parameter  $c$  180 as a site-specific metric of the centennially stable SOC fraction content. As already stated in Cécillon et al. (2018), in our view, the centennially stable SOC fraction is not biogeochemically inert; its mean age and mean residence time in soil are both assumed to be high (centuries), though not precisely defined here. As a result, its decline with time is negligible at the timescale of the long-term agricultural experiments or the long-term vegetation change site. We thus considered the centennially stable SOC fraction content at each experimental site to be constant. In this study, we used the centennially 185 stable SOC fraction content already estimated by Franko and Merbach (2017) for the site of Bad Lauchstädt (on the LTBF experiment started in 1988), and by Cécillon et al. (2018) for the sites of Versailles, Grignon, Rothamsted and Ultuna. We estimated the content of the centennially stable SOC fraction for Askov and La Cabaña sites using the same Bayesian curve-fitting method described by Cécillon et al. (2018). The Bayesian inference method was performed using Python 2.7 and the PyMC library (Patil et al., 2010).

190

For the second version of PARTY<sub>SOC</sub>, we aimed at reducing the potential bias towards an overestimation of the centennially 195 stable SOC fraction content at reference sites using the Eq. (1) (supplementary Table S1). This overestimation is possible at reference sites with an LTBF treatment, as SOC inputs to bare fallow topsoils are low but not null (e.g., Jenkinson and Coleman, 1994; Petersen et al., 2005). Similarly, C<sub>4</sub>-plant derived SOC inputs are possible after conversion to C<sub>3</sub> plants at the site of La Cabaña. We thus used the lowest observed total (sites with an LTBF treatment) or C<sub>4</sub>-plant derived (La Cabaña site) topsoil SOC content value as the best estimate of the centennially stable SOC fraction content in reference sites where this measured value was lower than the fitted value of the site-specific parameter  $c$  of Eq. (1).

## 2.2 Rock-Eval® thermal analysis of topsoil samples available from reference sites

Surface soil samples (0–10 cm to 0–30 cm depending on the site; see supplementary Table S2) were obtained from the seven 200 reference sites described in Sect. 2.1. As described in Cécillon et al. (2018), the first version of the PARTY<sub>SOC</sub> statistical model was based on a set of 118 topsoil samples corresponding to time series obtained from the soil archives of the sites of Rothamsted (12 samples from the LTBF treatment and eight samples from the adjacent long-term grassland treatment),



Ultuna (23 samples from the LTBF treatment and 11 samples from the associated long-term cropland treatments), Grignon (12 samples from the LTBF treatment, six samples from the LTBF plus straw amendment treatment and six samples from the LTBF plus composted straw amendment treatment) and Versailles (20 samples from the LTBF treatment and 20 samples from the LTBF plus manure amendment treatment). All 118 topsoil samples were previously analyzed using Rock-Eval® thermal analysis (Cécillon et al., 2018).

For the second version of the statistical model, 78 additional topsoil samples were provided by managers of the three new reference sites. Thirty-five topsoil samples were obtained from the soil archives of the Askov site (19 samples corresponding to different dates of the LTBF treatment and 16 samples corresponding to different dates of the associated long-term cropland treatments). Twenty-seven topsoil samples were obtained from the soil archives of the Bad Lauchstädt site (eight samples from two dates of the mechanical LTBF treatment, eight samples from two dates of the chemical LTBF treatment and eleven samples from two dates of several long-term cropland treatments of the static fertilization experiment, eight out of the latter coming from treatments with manure applications). Sixteen topsoil samples were obtained from the site of La Cabaña (13 samples from different C<sub>3</sub>-plant oil palm fields planted at different dates and three samples from different long-term C<sub>4</sub>-plant pastures).

The 78 additional topsoil samples from Askov, Bad Lauchstädt and La Cabaña were analyzed using the same Rock-Eval® 6 Turbo device (Vinci Technologies, France; see Behar et al., 2001 for a description of the apparatus) and the same setup as the one used for the sample set of the first version of the PARTY<sub>SOC</sub> statistical model, described by Cécillon et al. (2018). Briefly, *ca.* 60 mg of ground (< 250 µm) topsoil samples were subjected to sequential pyrolysis and oxidation phases. The Rock-Eval® pyrolysis phase was carried out in an N<sub>2</sub> atmosphere (3 min isotherm at 200 °C followed by a temperature ramp from 200 to 650 °C at a heating rate of 30 °C min<sup>-1</sup>). The Rock-Eval® oxidation phase was carried out in laboratory air atmosphere (1 min isotherm at 300 °C followed by a temperature ramp from 300 to 850 °C at a heating rate of 20 °C min<sup>-1</sup> and a final 5 min isotherm at 850 °C). Each Rock-Eval® analysis generated five thermograms corresponding to the volatile hydrocarbon effluents (HC\_PYR thermogram), CO (CO\_PYR thermogram) and CO<sub>2</sub> (CO<sub>2</sub>\_PYR thermogram) measured at each second during the pyrolysis phase, and to the CO (CO\_OX thermogram) and CO<sub>2</sub> (CO<sub>2</sub>\_OX thermogram) measured at each second during the oxidation phase (Behar et al., 2001).

A series of Rock-Eval® parameters were calculated from these five thermograms. For each thermogram, five temperature parameters (all in °C) were retained: T10, T30, T50, T70 and T90, which respectively represent the temperatures corresponding to the evolution of 10, 30, 50, 70 and 90% of the total amount of evolved gas. The calculation of Rock-Eval® temperature parameters was performed using different intervals of integration depending on the thermogram. The integration omitted the first 200 seconds of the analysis for the three thermograms of the pyrolysis phase. The integration ended at the time of analysis corresponding to the maximum oven temperatures of 650 °C (HC\_PYR thermogram), 560 °C (CO\_PYR



and CO2\_PYR thermograms), 850 °C (CO\_OX thermogram) and 611 °C (CO2\_OX thermogram). These intervals of integration prevented any interference by inorganic carbon from most soil carbonates, and they ensured comparability with previous studies (Barré et al., 2016; Cécillon et al., 2018; Poeplau et al., 2019; Soucémariandin et al., 2018b). Automatic 240 baseline correction (as calculated by the software of the Rock-Eval® apparatus; Vinci Technologies, France) was performed for all thermograms but the CO\_PYR and the CO2\_PYR thermograms. This correction can yield some negative values for the CO\_PYR and CO2\_PYR thermograms of soil samples with very low SOC content (data not shown). For the HC\_PYR thermogram we also determined three parameters reflecting a proportion of thermally resistant or labile hydrocarbons: a parameter representing the proportion of hydrocarbons evolved between 200 and 450 °C (thermo-labile hydrocarbons, 245 TLHC-index, unitless; modified from Saenger et al. (2013, 2015) as described by Cécillon et al. (2018); a parameter representing the preservation of thermally labile hydrocarbons (I-index, unitless, after Sebag et al., 2016); and a parameter representing the proportion of hydrocarbons thermally stable at 400 °C (R-index, unitless, after Sebag et al., 2016). We also 250 considered the hydrogen index (HI, mg HC g<sup>-1</sup> C) and oxygen index (OI<sub>RE6</sub>, mg O<sub>2</sub> g<sup>-1</sup> C) that respectively describe the relative elemental hydrogen and oxygen enrichment of soil organic matter (see *e.g.*, Barré et al., 2016). These 30 Rock-Eval® parameters are not directly related to total SOC content and were all included in the first version of the PARTY<sub>SOC</sub> 255 model developed by Cécillon et al. (2018).

In this second version of PARTY<sub>SOC</sub>, we considered ten additional Rock-Eval® parameters as possible predictors, some of 260 these being directly linked to SOC content (supplementary Table S1). These ten parameters were calculated for all the 196 topsoil samples available from the seven reference sites. They included: the content of SOC as determined by Rock-Eval® (TOC<sub>RE6</sub>, g C kg<sup>-1</sup>); the content of soil inorganic carbon as determined by Rock-Eval® (MinC, g C kg<sup>-1</sup>); the content of SOC evolved as HC, CO or CO<sub>2</sub> during the pyrolysis phase of Rock-Eval® (PC, g C kg<sup>-1</sup>); the content of SOC evolved as HC 265 during the temperature ramp (200–650 °C) of the pyrolysis phase of Rock-Eval® (S2, g C kg<sup>-1</sup>); the content of SOC that evolved as HC, CO or CO<sub>2</sub> during the first 200 seconds of the pyrolysis phase (at *ca.* 200 °C) of Rock-Eval® (PseudoS1, g C kg<sup>-1</sup>, after Khedim et al., 2020); the ratio of PseudoS1 to PC (PseudoS1/PC, unitless); the ratio of PseudoS1 to TOC<sub>RE6</sub> 270 (PseudoS1/TOC<sub>RE6</sub>, unitless); the ratio of S2 to PC (S2/PC, unitless, after Poeplau et al., 2019); the ratio of PC to TOC<sub>RE6</sub> (PC/TOC<sub>RE6</sub>, unitless); and the ratio of HI to OI<sub>RE6</sub> (HI/OI<sub>RE6</sub>, mg HC mg<sup>-1</sup> O<sub>2</sub>). TOC<sub>RE6</sub>, MinC, PC, HI and OI<sub>RE6</sub> were obtained as default parameters from the software of the Rock-Eval® apparatus (Vinci Technologies, France). All other 275 Rock-Eval® parameters were calculated from the integration of the five thermograms using R version 4.0.0 (R Core Team, 2020; RStudio Team, 2020) and functions from the R packages hyperSpec (Beleites and Sergo, 2020), pracma (Borchers, 2019) and stringr (Wickham, 2019).

### 2.3 Determination of the centennially stable SOC fraction proportion in topsoil samples from the reference sites

Following the first version of PARTY<sub>SOC</sub> (Cécillon et al., 2018), the proportion of the centennially stable SOC fraction in a topsoil sample of a reference site was calculated as the ratio of the site-specific centennially stable SOC fraction content (see



270 Sect. 2.1) to the SOC content of this particular sample. We thus assume that the centennially stable SOC fraction content in topsoils is the same in the various agronomical treatments of a reference site and that it remains constant within the time-period studied at each site.

275 While for the first version of  $\text{PARTY}_{\text{SOC}}$ , the proportion of the centennially stable SOC fraction in reference topsoils was calculated with SOC contents determined by elemental analysis ( $\text{SOC}_{\text{EA}}$ ), in this second version, we preferred the SOC content determined by Rock-Eval® (supplementary Table S1). The reason behind this choice was to link the Rock-Eval® parameters measured on a reference topsoil sample to a calculated proportion of the centennially stable SOC fraction that better reflected the organic carbon that actually evolved during its Rock-Eval® analysis. This choice was possible for reference topsoil samples for which Rock-Eval® analyses showed a good organic carbon yield ( $\text{TOC}_{\text{RE6}}$  divided by  $\text{SOC}_{\text{EA}}$ , 280 and multiplied by 100). This is generally the case for most soils, with typical organic carbon yields of Rock-Eval® ranging from 90 to 100% of  $\text{SOC}_{\text{EA}}$  (Disnar et al., 2003). For the topsoils of the sites of Grignon, Rothamsted, Ultuna and Versailles used in the first version of  $\text{PARTY}_{\text{SOC}}$ , the organic carbon yield of Rock-Eval® was greater than 96% (linear regression model,  $R^2 = 0.97$ ,  $n = 118$ ; Cécillon et al., 2018). Similarly, Rock-Eval® analyses of topsoil samples from the site of La Cabaña showed very good organic carbon yields (95% on average, linear regression model  $R^2 = 0.95$ ,  $n = 16$ ). For these five 285 reference sites (corresponding to 134 reference topsoil samples), we thus used the Rock-Eval® parameter  $\text{TOC}_{\text{RE6}}$  as a measure of the SOC content of topsoil samples to calculate their respective proportion of the centennially stable SOC fraction. Conversely, Rock-Eval® analyses of topsoil samples from the sites of Askov and Bad Lauchstädt showed moderate 290 organic carbon yields (90% on average for topsoils of Askov, with a noisy linear regression model  $R^2 = 0.68$ ,  $n = 30$ ; and 92% on average for topsoils of Bad Lauchstädt, yet with a very good linear regression model  $R^2 = 0.96$ ,  $n = 11$ ). Using the total carbon measured by Rock-Eval® (*i.e.*, the sum of  $\text{TOC}_{\text{RE6}}$  plus MinC Rock-Eval® parameters) as an estimate of the 295 SOC content of topsoil samples for these two sites —that are not carbonated— increased the organic carbon yield of Rock-Eval® analyses (96% on average at Askov, still with a noisy linear regression model  $R^2 = 0.66$ ,  $n = 30$ ; and 101% on average at Bad Lauchstädt, with a very good linear regression model  $R^2 = 0.95$ ,  $n = 11$ ). For the two reference sites of Askov and Bad Lauchstädt (corresponding to 62 topsoil samples), we thus used the sum of Rock-Eval® parameters  $\text{TOC}_{\text{RE6}}$  plus MinC as a measure of the SOC content of topsoil samples to calculate their proportion of the centennially stable SOC fraction.

300 The uncertainty in the proportion of the centennially stable SOC fraction was calculated using Equation 6 of the paper published by Cécillon et al. (2018), propagating the uncertainties in SOC content data (using a standard error of  $0.5 \text{ g C kg}^{-1}$ , following Barré et al., 2010) and in the site-specific contents of the centennially stable SOC fraction (see above and Table 1).



**Table 1: Main statistics of soil organic carbon contents, site-specific contents of the centennially stable SOC fraction, and resulting proportions of centennially stable SOC fraction in topsoils of the seven reference sites used as the reference topsoil sample sets of the  $\text{PARTY}_{\text{SOCv2.0}}$  and  $\text{PARTY}_{\text{SOCv2.0}_{\text{EU}}}$  models.** More details on agronomical treatments and sampling year of reference topsoil samples are provided in supplementary Table S3. Abbreviations: SOC, soil organic carbon; LTBF, long-term bare fallow; min, minimum; max, maximum; sd, standard deviation.

Reference site (Country)	Treatments (number of samples)	SOC content (g C kg <sup>-1</sup> )	Centennially stable SOC fraction content (g C kg <sup>-1</sup> )	Proportion of the centennially stable SOC fraction (unitless)
		mean (min, max, sd)	mean (sd)	mean (min, max, sd)
		measurement method	estimation method	
<b>Versailles</b> (France)	LTBF (n = 15)	10.4 (5.6, 17.9, 3.9) TOC <sub>RE6</sub>	5.50 (0.50) Lowest SOC <sub>EA</sub> measured on site	0.60 (0.31, 0.98, 0.20)
<b>Rothamsted</b> (England)	Grassland (n = 7) LTBF (n = 8)	28.3 (12.2, 41.5, 10.1) TOC <sub>RE6</sub>	9.72 (0.50) Lowest SOC <sub>EA</sub> measured on site	0.40 (0.23, 0.80, 0.18)
<b>Ultuna</b> (Sweden)	Cropland (n = 3; +straw n = 8) LTBF (n = 4)	15.2 (10.0, 20.3, 2.8) TOC <sub>RE6</sub>	6.95 (0.88) Bayesian curve-fitting	0.47 (0.34, 0.70, 0.09)
<b>Grignon</b> (France)	LTBF (n = 12, +straw n = 3)	11.5 (8, 14.3, 1.7) TOC <sub>RE6</sub>	7.12 (1.00) Bayesian curve-fitting	0.63 (0.50, 0.89, 0.10)
<b>Askov</b> (Denmark)	Cropland (n = 7) LTBF (n = 8)	13.8 (11.1, 16.8, 1.9) TOC <sub>RE6</sub> +MinC	5.10 (0.88) Bayesian curve-fitting	0.38 (0.30, 0.46, 0.05)
<b>Bad Lauchstädt</b> (Germany)	Cropland (n = 1) LTBF (n = 14)	18.0 (16.8, 19.4, 0.6) TOC <sub>RE6</sub> +MinC	15.00 (0.50) Lowest SOC <sub>EA</sub> measured on site	0.84 (0.77, 0.89, 0.03)
<b>La Cabaña</b> (Colombia)	Pasture (n = 3) Oil-palm plantation (n = 12)	17.8 (10.2, 31.8, 5.7) TOC <sub>RE6</sub>	4.75 (0.50) Lowest SOC <sub>EA</sub> measured on site	0.29 (0.15, 0.47, 0.10)
<b>Reference soil sample set of <math>\text{PARTY}_{\text{SOCv2.0}}</math> (n = 105)</b>		16.4 (5.6, 41.5, 7.3)		0.52 (0.15, 0.98, 0.21)
<b>Reference soil sample set of <math>\text{PARTY}_{\text{SOCv2.0}_{\text{EU}}}</math> (n = 90)</b>		16.2 (5.6, 41.5, 7.5)		0.55 (0.23, 0.98, 0.20)



## 2.4 Selection of the learning set and of meaningful Rock-Eval® predictors variables for the PARTY<sub>SOCv2.0</sub> model

In machine-learning, the selection of the learning set (here, the training and test sets of reference topsoil samples) of the 310 model influences the performances of the model, just like the selection of the predictor variables (here, the Rock-Eval® parameters) (e.g., Cécillon et al., 2008; Wehrens, 2020).

For this second version of PARTY<sub>SOC</sub>, we changed some criteria regarding the inclusion of the available reference topsoil 315 samples in the learning set of the model (supplementary Table S1). We excluded from the learning set all the topsoil samples experiencing agronomical treatments that may have changed the site-specific content of the centennially stable SOC fraction.

These agronomical treatments concern the repeated application of some types of exogenous organic matter such as compost 320 or manure, for which we suspect that they may increase the content of the centennially stable SOC fraction after several decades. Therefore, to increase the likelihood of verifying our hypothesis of a constant content of the centennially stable SOC fraction at each reference site in time and space (see Sect. 2.3), we excluded all reference topsoil samples experiencing repeated applications of composted straw (six samples from Grignon), or manure (20 samples from Versailles and eight samples from Bad Lauchstädt) from the learning set of the statistical model. Yet, we kept some reference topsoil samples from Grignon and Ultuna experiencing repeated applications of straw.

We also excluded from the learning set of the model the reference topsoil samples for which the organic carbon yield of 325 Rock-Eval® is below 86% or above 116%. For the site of Askov with a noisy relationship between SOC<sub>EA</sub> and the sum TOC<sub>RE6</sub> plus MinC (see Sect. 2.3), we excluded the five samples without a SOC<sub>EA</sub> measurement preventing the calculation of the organic carbon yield of their Rock-Eval® analysis. Conversely, for the site of Bad Lauchstädt we kept topsoil samples 330 without available SOC<sub>EA</sub> measurements, as the linear relationship between SOC<sub>EA</sub> and the sum TOC<sub>RE6</sub> plus MinC was very good for this site (see Sect. 2.3). These criteria regarding the organic carbon yield of Rock-Eval® lead to the exclusion of nine samples from the site of Askov, four additional samples from the site of Versailles and two from the site of Ultuna.

Contrary to the first version of PARTY<sub>SOC</sub> (Cécillon et al., 2018), this second version is based on a balanced contribution of 335 each reference site to the statistical model (supplementary Table S1). Each reference site contributes to the model with 15 samples, so that the reference sample set of the PARTY<sub>SOCv2.0</sub> statistical model is composed of 105 topsoil samples (90 for the European version of the model PARTY<sub>SOCv2.0\_EU</sub>). Besides the above-mentioned exclusion criteria (that excluded 49 out of the 196 topsoil samples available from the seven reference sites), the 15 topsoil samples retained for each reference site were selected: (1) to have a range of proportion of centennially stable SOC fraction as wide as possible; (2) to have the best organic carbon yield of Rock-Eval® analysis. On average, the organic carbon yield of the Rock-Eval® analyses for the retained learning set of reference topsoil samples (calculated as described above) was greater than 98% of SOC<sub>EA</sub> 340 (SOC<sub>DETERMINED\_BY\_ROCK-EVAL®</sub> = 0.9924 SOC<sub>EA</sub> - 0.1051, R<sup>2</sup> = 0.99, n = 91 topsoil samples with available SOC<sub>EA</sub>



measurements). The list of the 105 reference topsoil samples retained as the learning set of  $\text{PARTY}_{\text{SOCv}2.0}$  is provided in supplementary Table S3. This list includes, for each reference topsoil sample, information on its reference site, land cover, agronomical treatment, sampling year and its values for the 40 Rock-Eval® parameters.

345 The 40 Rock-Eval® parameters calculated (see Sect. 2.2) captured most of the information related to SOC thermal stability, elemental stoichiometry and content that is contained in the five Rock-Eval® thermograms. However, not all Rock-Eval® parameters do necessarily carry meaningful information for partitioning SOC into its centennially stable and active fractions (Cécillon et al., 2018). The  $\text{PARTY}_{\text{SOCv}2.0}$  statistical model and its European version  $\text{PARTY}_{\text{SOCv}2.0_{\text{EU}}}$  incorporate as predictor variables only the Rock-Eval® parameters showing a strong relationship with the proportion of the centennially stable SOC fraction (supplementary Table S1). The absolute value of 0.50 for the Spearman's rho (nonparametric and nonlinear correlation test) was used as a threshold to select meaningful Rock-Eval® predictor variables (calculated on the reference topsoil sample set of the  $\text{PARTY}_{\text{SOCv}2.0}$  model,  $n = 105$ ). Basic statistics of all Rock-Eval® parameters (learning set of  $\text{PARTY}_{\text{SOCv}2.0}$ ) are reported in supplementary Table S4.

355 **2.5 Random forests regression models to predict the proportion of the centennially stable SOC fraction from Rock-Eval® parameters, performance assessment and error propagation in the statistical models**

The  $\text{PARTY}_{\text{SOCv}2.0}$  statistical model consists of a nonparametric and nonlinear multivariate regression model relating the proportion of the centennially stable SOC fraction (response vector or dependent variable  $\mathbf{y}$ ) of the reference soil sample set ( $n = 105$  topsoil samples from the seven reference sites, see Sect. 2.4) to their Rock-Eval® parameters summarized by a matrix of predictor variables ( $\mathbf{X}$ ) made up of the selected centered and scaled Rock-Eval® parameters. As stated above, we 360 also built a regional (European) version of the statistical model based on the six European reference sites only ( $\text{PARTY}_{\text{SOCv}2.0_{\text{EU}}}$ , using the 90 reference topsoil samples from Askov, Bad Lauchstädt, Grignon, Rothamsted, Ultuna and Versailles).

365 Like the first version of the  $\text{PARTY}_{\text{SOC}}$  statistical model, this second version uses the machine-learning algorithm of random forests-random inputs (hereafter termed random forests) proposed by Breiman (2001). This algorithm aggregates a collection of random regression trees (Breiman, 2001; Genuer and Poggi, 2020). The  $\text{PARTY}_{\text{SOCv}2.0}$  and its European version  $\text{PARTY}_{\text{SOCv}2.0_{\text{EU}}}$  are based on a forest of 1000 different regression trees made of splits and nodes. The learning algorithm of random forests combines bootstrap resampling and random variable selection. Each of the 1000 regression trees was grown on a bootstrapped subset of the reference topsoil sample set (*i.e.*, containing *ca.* two-thirds of “in-bag” samples). The 370 algorithm randomly sampled one-third out of the selected Rock-Eval® parameters (see Sect. 2.4) as candidates at each split of the regression tree, and it used a minimum size of terminal tree nodes of five topsoil samples. The relative importance (*i.e.*, ranking) of each selected Rock-Eval® parameters in the regression models was computed as the unscaled permutation accuracy (Strobl et al., 2009).



375 The performance of the  $\text{PARTY}_{\text{SOCv}2.0}$  and the  $\text{PARTY}_{\text{SOCv}2.0_{\text{EU}}}$  random forests regression models was assessed by statistical metrics comparing the predicted *vs.* the estimated values of their reference topsoil sample set using three different strategies. First, the predictive ability of both models was assessed by an “internal” procedure that used their respective whole reference topsoil sample sets ( $n = 105$  samples for  $\text{PARTY}_{\text{SOCv}2.0}$ ,  $n = 90$  samples for  $\text{PARTY}_{\text{SOCv}2.0_{\text{EU}}}$ ). For this procedure, performance statistics were calculated only on the “out-of-bag” topsoil samples of the whole reference sets, using  
380 a random seed of 1 to initialize the pseudorandom number generator of the R software. Out-of-bag samples are observations from the training sets not included in the learning topsoil sample set for a specific regression tree that can be used as a “built-in” test set for calculating its prediction accuracy (Strobl et al., 2009). Second, the predictive ability of the models was assessed by a “random splitting” procedure that split randomly their respective reference topsoil sample sets into a test set (made of  $n = 30$  samples), and a training set ( $n = 75$  samples for  $\text{PARTY}_{\text{SOCv}2.0}$ ,  $n = 60$  samples for  $\text{PARTY}_{\text{SOCv}2.0_{\text{EU}}}$ ). This  
385 procedure was repeated 15 times using random seeds from 1 to 15 in the R software. Third, a fully independent “leave-one-site-out” procedure was used to assess the predictive ability of the models. This procedure successively excluded topsoil samples of one reference site from the training set and uses them as a test set ( $n = 15$ ) for the models. It used the random seed of 1 in the R software. For the second and third procedures, performance statistics were calculated (1) on the “out-of-bag” topsoil samples of the training sets and (2) on the topsoil samples of the test sets.

390

Finally, the sensitivity of model performance to the reference sites included in the learning set of the random forests regression model was assessed on independent soils from two reference sites, used as examples. For this sensitivity analysis, topsoil samples from Grignon and Versailles ( $n = 15$  samples) were successively used as fully independent test sets for several random forests regression models. Combinations of topsoil samples from a decreasing number of the remaining  
395 reference sites were selected as training sets for the models, on the basis of their potential proximity to the topsoil samples of the test sets, regarding their pedological or climatic conditions. The size of the various training sets composed for the sensitivity analysis ranged from  $n = 90$  samples (six training reference sites) to  $n = 30$  samples (only two training reference sites).

400 Several statistics were used to assess the predictive ability of the regression models. The coefficient of determination:  $R^2_{\text{OOB}}$ , calculated on the “out-of-bag” samples of the training sets; and  $R^2$ , calculated on the samples of the test sets. The root-mean-square error of prediction:  $\text{RMSEP}_{\text{OOB}}$ , calculated on the “out-of-bag” samples of the training sets; and  $\text{RMSEP}$ , calculated on the samples of the test sets. The relative  $\text{RMSEP}$ :  ${}_R\text{RMSEP}$ , calculated as the ratio of the  $\text{RMSEP}$  to the mean value of the test sets. The ratio of performance to interquartile range (RPIQ) was calculated as the ratio of the interquartile range of the  
405 test sets ( $Q3 - Q1$ ; which gives the range accounting for 50% of the test sets around its median value) to the  $\text{RMSEP}$  (Bellon-Maurel et al., 2010). The bias of the random forests regression models was calculated as the mean of the model predictions on the test sets minus the actual mean of the test sets. Additionally, site-specific  $\text{RMSEP}$  and  ${}_R\text{RMSEP}$  were calculated for



the “leave-one-site-out” procedure (on the 15 independent test topsoil samples from each site). The uncertainty on the model predictions for new topsoils was determined using a methodology that was fully described by Cécillon et al. (2018). This  
410 methodology was adapted after the work of Coulston et al. (2016), to explicitly take into account the uncertainty in the reference values of the proportion of the centennially stable SOC fraction (see Sect. 2.3) that were used to build the models (Cécillon et al., 2018).

PARTY<sub>SOC</sub>v2.0 and PARTY<sub>SOC</sub>v2.0<sub>EU</sub> were programmed as R scripts in the RStudio environment software (RStudio Team, 415 2020), and were run using the R version 4.0.0 (R Core Team, 2020). The R scripts use the random forests algorithm of the randomForest R package (Liaw and Wiener, 2002) and the boot R package for bootstrapping (Canty and Ripley, 2020; Davison and Hinkley, 1997).

### 3 Results

#### 3.1 Content of the centennially stable SOC fraction at the reference sites

420 The two newly fitted values of the centennially stable SOC fraction content (*i.e.*, parameter  $c$  in Eq. (1), see Sect. 2.1) were 5.10 g C kg<sup>-1</sup> at the site of Askov (standard deviation = 0.88 g C kg<sup>-1</sup>) and 5.12 g C kg<sup>-1</sup> at the site of La Cabaña (standard deviation = 0.35 g C kg<sup>-1</sup>). The fitted values of parameter  $c$  in Eq. (1) for all reference sites and their standard errors are provided in supplementary Table S2. A total (reference sites with an LTBF treatment) or a C<sub>4</sub>-plant derived (La Cabaña site) SOC content value lower than the fitted value of the site-specific parameter  $c$  in Eq. (1) was measured in four out the seven  
425 reference sites of the PARTY<sub>SOC</sub>v2.0 model. At Bad Lauchstädt, a SOC<sub>EA</sub> value of 15.0 g C kg<sup>-1</sup> was reported by Körschens et al. (1998) for topsoils of the well ring experiment (Ansorge, 1966). At Rothamsted, a SOC<sub>EA</sub> measurement of 9.72 g C kg<sup>-1</sup> was reported for topsoils of the Highfield LTBF experiment by Cécillon et al. (2018). At Versailles a SOC<sub>EA</sub> measurement of 5.50 g C kg<sup>-1</sup> was reported after 80 years of bare fallow by Barré et al. (2010). At La Cabaña, a C<sub>4</sub>-plant derived SOC content of 4.75 g C kg<sup>-1</sup> was calculated using data from Quezada et al. (2019). These values were thus retained as the best  
430 estimates of the site-specific content of the centennially stable SOC fraction in topsoils of the four sites (Table 1). As these site-specific values of the centennially stable SOC fraction content were derived from SOC<sub>EA</sub> measurements, we attributed a standard deviation of 0.50 g C kg<sup>-1</sup> to each of them, following Barré et al. (2010). The final estimates of the content of the centennially stable SOC fraction at the seven reference sites that were used in the PARTY<sub>SOC</sub>v2.0 statistical model are provided in Table 1. They varied by a factor of three across the reference sites, ranging from 4.75 g C kg<sup>-1</sup> at La Cabaña to  
435 15.00 g C kg<sup>-1</sup> at Bad Lauchstädt. The lowest value of the topsoil content of the centennially stable SOC fraction used in the European version PARTY<sub>SOC</sub>v2.0<sub>EU</sub> of the statistical model differed only slightly from the one of the PARTY<sub>SOC</sub>v2.0 model (5.10 g C kg<sup>-1</sup> at the site of Askov).



### 3.2 Content and biogeochemical stability of SOC in the learning sets, and selection of meaningful Rock-Eval® parameters as predictor variables for the $\text{PARTY}_{\text{SOCv2.0}}$ and $\text{PARTY}_{\text{SOCv2.0}_{\text{EU}}}$ models

440 The SOC content in the topsoil samples of the seven reference sites ranged from 5.6 to 41.5 g C kg<sup>-1</sup> in the learning sets of the  $\text{PARTY}_{\text{SOCv2.0}}$  (n = 105) and  $\text{PARTY}_{\text{SOCv2.0}_{\text{EU}}}$  (n = 90) models (Table 1). As showed in Table 1, this resulted in proportions of the centennially stable SOC fraction ranging from 0.15 to 0.98 ( $\text{PARTY}_{\text{SOCv2.0}}$  learning set), and from 0.23 to 0.98 ( $\text{PARTY}_{\text{SOCv2.0}_{\text{EU}}}$  learning set). All the 25 calculated Rock-Eval® temperature parameters showed positive values of Spearman's rho coefficient with the response variable of the  $\text{PARTY}_{\text{SOCv2.0}}$  model (n = 105; with Spearman's rho values up to 0.81 for  $T90_{\text{HC\_PYR}}$ ; Table 2). While the inorganic carbon content was not correlated to the proportion of the centennially stable SOC fraction,  $\text{TOC}_{\text{RE6}}$  was significantly and negatively correlated to the response variable of the  $\text{PARTY}_{\text{SOCv2.0}}$  model (Spearman's rho = -0.55; Table 2). Other Rock-Eval® parameters linked to soil carbon content showed a stronger relationship than  $\text{TOC}_{\text{RE6}}$  with the proportion of the centennially stable SOC fraction. This was the case for S2 and PC that showed the highest absolute Spearman's rho coefficients, with a highly significant negative relationship (Spearman's rho = -0.85; Table 2). Eighteen out of the 40 calculated Rock-Eval® parameters showed an absolute value of Spearman's rho above 0.5 with the proportion of the centennially stable SOC fraction in the learning set of the  $\text{PARTY}_{\text{SOCv2.0}}$  model (n = 105; Table 2), and were thus retained as predictor variables for the models. The 18 Rock-Eval® parameters retained were: the Rock-Eval® temperature parameters  $T70_{\text{HC\_PYR}}$ ,  $T90_{\text{HC\_PYR}}$ ,  $T30_{\text{CO}_2\text{\_PYR}}$ ,  $T50_{\text{CO}_2\text{\_PYR}}$ ,  $T70_{\text{CO}_2\text{\_PYR}}$ ,  $T90_{\text{CO}_2\text{\_PYR}}$ ,  $T70_{\text{CO\_OX}}$ ,  $T50_{\text{CO}_2\text{\_OX}}$ ,  $T70_{\text{CO}_2\text{\_OX}}$ ,  $T90_{\text{CO}_2\text{\_OX}}$ , and the Rock-Eval® parameters  $\text{PseudoS1}$ ,  $\text{S2}$ ,  $\text{S2/PC}$ ,  $\text{HI}$ ,  $\text{HI/OI}_{\text{RE6}}$ ,  $\text{PC}$ ,  $\text{PC/TOC}_{\text{RE6}}$ , and 455  $\text{TOC}_{\text{RE6}}$ .

460 **Table 2: Spearman's rank correlation coefficient test between the 40 calculated Rock-Eval® parameters and the proportion of the centennially stable organic carbon fraction in the reference topsoil sample set of the  $\text{PARTY}_{\text{SOCv2.0}}$  model (n = 105), and variable importance (ranking) of the 18 selected Rock-Eval® parameters for predicting the proportion of the centennially stable SOC fraction in the  $\text{PARTY}_{\text{SOCv2.0}}$  and  $\text{PARTY}_{\text{SOCv2.0}_{\text{EU}}}$  random forests regression models.** Symbols for p-values: \*\*\* p < 0.001; \*\* p < 0.01; \* p < 0.05; NS p > 0.05 = not significant. See Section 2.2 for a description of the units of the 40 Rock-Eval® parameters. The 18 Rock-Eval® parameters retained as predictor variables for the second version of  $\text{PARTY}_{\text{SOC}}$  are shown in bold. Abbreviation: SOC, soil organic carbon.

Rock-Eval® parameter	Spearman's p with the proportion of the centennially stable SOC fraction	p-value	Variable importance to predict the proportion of the centennially stable SOC fraction in the $\text{PARTY}_{\text{SOCv2.0}}$ regression model (rank)	Variable importance to predict the proportion of the centennially stable SOC fraction in the $\text{PARTY}_{\text{SOCv2.0}_{\text{EU}}}$ regression model (rank)
$T10_{\text{HC\_PYR}}$	0.38	0.0001	NA	NA



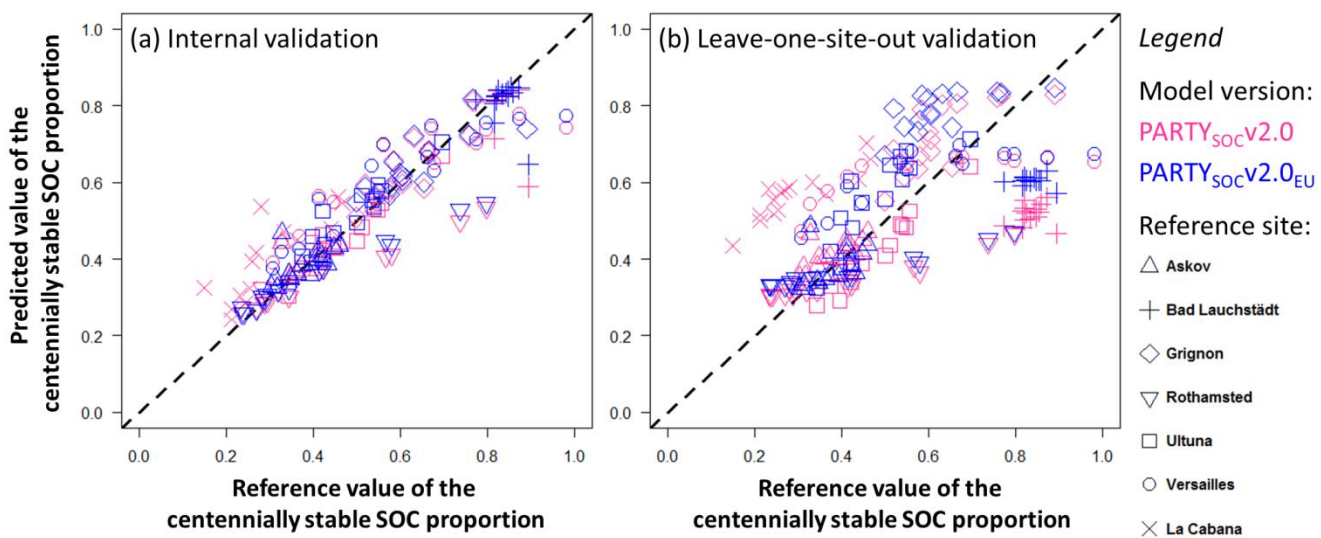
T30 <sub>HC</sub> _PYR	0.47	0.0000	NA	NA
T50 <sub>HC</sub> _PYR	0.46	0.0000	NA	NA
<b>T70<sub>HC</sub>_PYR</b>	<b>0.54</b>	<b>0.0000</b>	<b>17</b>	<b>15</b>
<b>T90<sub>HC</sub>_PYR</b>	<b>0.81</b>	<b>0.0000</b>	<b>5</b>	<b>13</b>
T10 <sub>CO</sub> _PYR	0.40	0.0000	NA	NA
T30 <sub>CO</sub> _PYR	0.36	0.0001	NA	NA
T50 <sub>CO</sub> _PYR	0.33	0.0005	NA	NA
T70 <sub>CO</sub> _PYR	0.31	0.0014	NA	NA
T90 <sub>CO</sub> _PYR	0.31	0.0013	NA	NA
T10 <sub>CO2</sub> _PYR	0.35	0.0003	NA	NA
<b>T30<sub>CO2</sub>_PYR</b>	<b>0.56</b>	<b>0.0000</b>	<b>12</b>	<b>10</b>
<b>T50<sub>CO2</sub>_PYR</b>	<b>0.55</b>	<b>0.0000</b>	<b>8</b>	<b>2</b>
<b>T70<sub>CO2</sub>_PYR</b>	<b>0.55</b>	<b>0.0000</b>	<b>10</b>	<b>7</b>
<b>T90<sub>CO2</sub>_PYR</b>	<b>0.58</b>	<b>0.0000</b>	<b>11</b>	<b>11</b>
T10 <sub>CO</sub> _OX	0.31	0.0013	NA	NA
T30 <sub>CO</sub> _OX	0.41	0.0000	NA	NA
T50 <sub>CO</sub> _OX	0.49	0.0000	NA	NA
<b>T70<sub>CO</sub>_OX</b>	<b>0.58</b>	<b>0.0000</b>	<b>9</b>	<b>16</b>
T90 <sub>CO</sub> _OX	0.33	0.0007	NA	NA
T10 <sub>CO2</sub> _OX	0.10	0.3349	NA	NA
T30 <sub>CO2</sub> _OX	0.39	0.0000	NA	NA
<b>T50<sub>CO2</sub>_OX</b>	<b>0.63</b>	<b>0.0000</b>	<b>13</b>	<b>14</b>
<b>T70<sub>CO2</sub>_OX</b>	<b>0.70</b>	<b>0.0000</b>	<b>4</b>	<b>12</b>
<b>T90<sub>CO2</sub>_OX</b>	<b>0.60</b>	<b>0.0000</b>	<b>14</b>	<b>17</b>
I-index	-0.40	0.0000	NA	NA
R-index	0.47	0.0000	NA	NA
TLHC-index	-0.49	0.0000	NA	NA
<b>HI</b>	<b>-0.72</b>	<b>0.0000</b>	<b>7</b>	<b>6</b>
OI <sub>RE6</sub>	-0.09	0.3504	NA	NA
<b>TOC<sub>RE6</sub></b>	<b>-0.55</b>	<b>0.0000</b>	<b>6</b>	<b>9</b>
MinC	0.03	0.7430	NA	NA
PC	<b>-0.85</b>	<b>0.0000</b>	<b>2</b>	<b>3</b>
S2	<b>-0.85</b>	<b>0.0000</b>	<b>1</b>	<b>1</b>



<b>PseudoS1</b>	<b>-0.50</b>	<b>0.0000</b>	<b>18</b>	<b>18</b>
PseudoS1/PC	0.28	0.0033	NA	NA
PseudoS1/TOC <sub>RE6</sub>	-0.06	0.5702	NA	NA
<b>S2/PC</b>	<b>-0.70</b>	<b>0.0000</b>	<b>16</b>	<b>4</b>
<b>PC/TOC<sub>RE6</sub></b>	<b>-0.71</b>	<b>0.0000</b>	<b>3</b>	<b>8</b>
<b>HI/OI<sub>RE6</sub></b>	<b>-0.68</b>	<b>0.0000</b>	<b>15</b>	<b>5</b>

465 **3.3 Performance assessment of the  $\text{PARTY}_{\text{SOCv2.0}}$  and  $\text{PARTY}_{\text{SOCv2.0}_{\text{EU}}}$  statistical models**

Using both the “internal” and the “random splitting” performance assessment procedures (see Sect. 2.5), the  $\text{PARTY}_{\text{SOCv2.0}}$  and  $\text{PARTY}_{\text{SOCv2.0}_{\text{EU}}}$  models showed good to very good predictive ability of the proportion of the centennial stable SOC fraction (Fig. 2a; Table 3a). For most of the calculated statistics, the European version of the model  $\text{PARTY}_{\text{SOCv2.0}_{\text{EU}}}$  showed better performances than the  $\text{PARTY}_{\text{SOCv2.0}}$  model (Table 3). Using the “random splitting” procedure, the mean  $R^2$  470 of  $\text{PARTY}_{\text{SOCv2.0}_{\text{EU}}}$  was 0.87 (0.81 for  $\text{PARTY}_{\text{SOCv2.0}}$ ), its RMSEP and  $_{\text{R}}\text{RMSEP}$  were respectively 0.07 and 0.13 (0.09 and 0.17 for  $\text{PARTY}_{\text{SOCv2.0}}$ ), and its mean RPIQ was 4.6 (3.6 for  $\text{PARTY}_{\text{SOCv2.0}}$ ). The bias was low for both models (Table 3a).



475 **Figure 2: Performance of the  $\text{PARTY}_{\text{SOCv2.0}}$  and the  $\text{PARTY}_{\text{SOCv2.0}_{\text{EU}}}$  statistical models based on Rock-Eval® thermal analysis for predicting the centennial stable organic carbon proportion in topsoils.** (a) Results of the internal validation procedure; (b) Results of the leave-one-site-out validation procedure (see Section 2.5 for more details on model performance assessment). Abbreviation: SOC, soil organic carbon.



Table 3: Performance of the  $\text{PARTY}_{\text{SOCv2.0}}$  and the  $\text{PARTY}_{\text{SOCv2.0}_{\text{EU}}}$  random forests regression models based on  
 480 Rock-Eval® thermal analysis for predicting the proportion of the centennially stable organic carbon fraction in  
 topsoils. (a) Performance statistics calculated for the internal, random splitting (mean statistics of 15 different models) and  
 leave-one-site-out validation procedures; (b) Site-specific performance statistics calculated for the leave-one-site-out  
 validation procedure. The performance statistics and their abbreviations are defined at Section 2.5.

(a)	Internal procedure		Random splitting procedure		Leave-one-site-out procedure	
	$\text{PARTY}_{\text{SOCv2.0}}$	$\text{PARTY}_{\text{SOCv2.0}_{\text{EU}}}$	$\text{PARTY}_{\text{SOCv2.0}}$	$\text{PARTY}_{\text{SOCv2.0}_{\text{EU}}}$	$\text{PARTY}_{\text{SOCv2.0}}$	$\text{PARTY}_{\text{SOCv2.0}_{\text{EU}}}$
$\text{R}^2_{\text{OOB}}$	0.83	0.87	0.80	0.84	-	-
$\text{RMSEP}_{\text{OOB}}$	0.08	0.07	0.09	0.08	-	-
$\text{R}^2$	-	-	0.81	0.87	0.23	0.45
$\text{RMSEP}$	-	-	0.09	0.07	0.18	0.15
$\text{R}^2_{\text{RMSEP}}$	-	-	0.17	0.13	0.36	0.27
$\text{RPIQ}$	-	-	3.59	4.60	1.75	2.39
Bias	-	-	0.005	0.006	< 0.001	-0.003

(b)	Leave-one-site-out procedure							
	Test set	Askov	Bad	Grignon	Versailles	Rothamsted	Ultuna	La Cabaña
Lauchstädt								
$\text{PARTY}_{\text{SOCv2.0}}$	Site-specific	0.05	0.32	0.11	0.17	0.14	0.06	0.28
	RMSEP							
	Site-specific	0.13	0.38	0.18	0.28	0.36	0.13	0.94
	$^2_{\text{RMSEP}}$							
$\text{PARTY}_{\text{SOCv2.0}_{\text{EU}}}$	Site-specific	0.05	0.23	0.18	0.14	0.14	0.09	-
	RMSEP							
	Site-specific	0.13	0.28	0.28	0.24	0.35	0.20	-
	$^2_{\text{RMSEP}}$							



The predictive ability of both models decreased when assessed using the “leave-one-site-out” procedure (see Sect. 2.5; Fig. 2b). Again,  $\text{PARTY}_{\text{SOCv2.0}_{\text{EU}}}$  showed better performance statistics than the  $\text{PARTY}_{\text{SOCv2.0}}$  model (Table 3; Fig. 2b), with an  $R^2$  of 0.45, an RMSEP of 0.15, an  $R_{\text{RMSEP}}$  of 0.27 and an RPIQ of 2.4. The  $\text{PARTY}_{\text{SOCv2.0}}$  model poorly predicted the proportion of the centennial stable SOC fraction in topsoil samples of two sites (Table 3b; Fig. 2b): La Cabaña (overestimation; with a site-specific RMSEP of 0.28) and Bad Lauchstädt (underestimation; with a site-specific RMSEP of 0.32). The proportion of the centennial stable SOC fraction in topsoil samples of Bad Lauchstädt remained underpredicted by the  $\text{PARTY}_{\text{SOCv2.0}_{\text{EU}}}$  model, though with a reduced site-specific RMSEP (0.23; Table 3b; Fig. 2b). All other site-specific RMSEPs were below 0.18 (0.17 at Versailles for  $\text{PARTY}_{\text{SOCv2.0}}$ , 0.18 at Grignon for  $\text{PARTY}_{\text{SOCv2.0}_{\text{EU}}}$ ; Table 3b), with remarkably low site-specific RMSEPs for the sites of Askov (below 0.05 for both models) and Ultuna (0.06 for  $\text{PARTY}_{\text{SOCv2.0}}$ ; 0.09 for  $\text{PARTY}_{\text{SOCv2.0}_{\text{EU}}}$ ).

The most important Rock-Eval® parameter for predicting the proportion of the centennial stable SOC fraction is S2 for both  $\text{PARTY}_{\text{SOCv2.0}}$  and  $\text{PARTY}_{\text{SOCv2.0}_{\text{EU}}}$  statistical models (Table 2). Conversely, the two models show only two Rock-Eval® parameters in common out of their five most important ones that are S2, PC, PC/TOC<sub>RE6</sub>, T70<sub>CO2\_OX</sub>, T90<sub>HC\_PYR</sub> for  $\text{PARTY}_{\text{SOCv2.0}}$  and S2, T50<sub>CO2\_PYR</sub>, PC, S2/PC, HI/OI<sub>RE6</sub> for  $\text{PARTY}_{\text{SOCv2.0}_{\text{EU}}}$  (Table 2).

### 3.4 Sensitivity of model performance to the reference sites included in the learning set

Restricting the learning set of the machine-learning model to topsoil samples from fewer reference sites with pedoclimatic conditions closer to the ones of a fully independent test site changed its performances (Fig. 3). Removing the reference sites with a climate (*i.e.*, La Cabaña) or a soil type (*i.e.*, Bad Lauchstädt) differing strongly from the independent test site (here, Grignon or Versailles used as examples) reduced the site-specific RMSEP and  $R_{\text{RMSEP}}$  of the model (supplementary Table S5). When Grignon or Versailles were used as independent test sites, the statistical model with the best predictive ability (*i.e.*, the lowest site-specific RMSEP and  $R_{\text{RMSEP}}$ ) used a learning set composed of 45 topsoil samples from three European reference sites (including the French site with the closest climate, despite its different soil type; supplementary Table S2 and S5; Fig. 3).

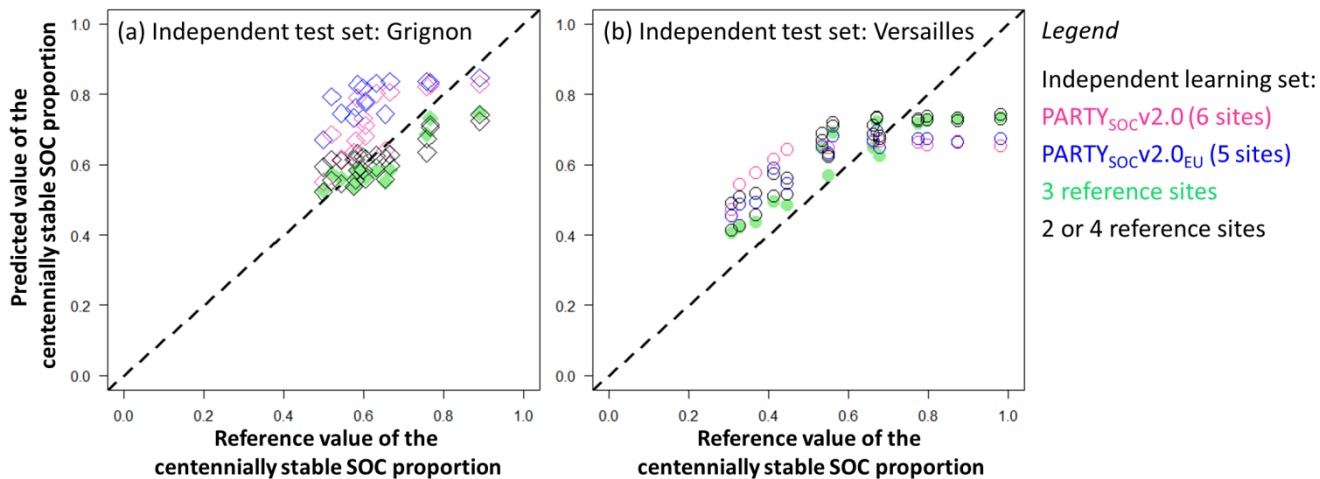


**Figure 3: Sensitivity of model performance to the reference sites included in the learning set, using 15 topsoil samples from the sites of (a) Grignon or (b) Versailles as independent test sets.** Predictions by statistical models showing the

515 lowest RMSEP and  $_{\text{R}}\text{RMSEP}$  are plotted in green (using a learning set composed of three independent reference sites to predict Grignon or Versailles as test set). See supplementary Table S5 for more details on the learning sets of the different statistical models and their site-specific performance statistics. Abbreviation: SOC, soil organic carbon.



## 4 Discussion

The second version of the PARTY<sub>SOC</sub> model incorporates a large number of modifications and improvements (supplementary Table S1), and its predictive ability was more thoroughly assessed compared to the first version of the statistical model (Cécillon et al., 2018). The critical examination of the performance of PARTY<sub>SOCv2.0</sub> and 525 PARTY<sub>SOCv2.0\_EU</sub> provides new insights: (1) on the relationships between Rock-Eval® parameters and the century-scale persistence of SOC; (2) on both current and potential capabilities of the model to partition the centennial stable and active organic carbon fraction in topsoils. Based on those insights, (3) we plan future expansions of the PARTY<sub>SOC</sub> global model, and we recommend the application of PARTY<sub>SOCv2.0\_EU</sub> in European agricultural topsoils to provide accurate information on SOC kinetic pools partitioning that may improve the simulations of simple models of SOC dynamics.

### 530 4.1 Rock-Eval® chemical and thermal information are related to the century-scale persistence of SOC

The methodology used to estimate the centennial stable SOC proportion in reference topsoils has been revised for the second version of the PARTY<sub>SOC</sub> model (see Sect. 2.1 and 2.3 and supplementary Table S1), and the learning set now integrates a wider range of centennial stable SOC contents [4.75–15.00 g C kg<sup>-1</sup>] with a median value of 6.95 g C kg<sup>-1</sup> (n = 7; Table 1). This range covers most of the published size estimates of this fraction in topsoils, estimated using different 535 methods (Balesdent et al., 1988; Barré et al., 2010; Buyanovsky and Wagner, 1998b; Cécillon et al., 2018; Franko and Merbach, 2017; Hsieh, 1992; Huggins et al., 1998; Jenkinson and Coleman, 1994; Körschens et al., 1998; Rühlmann, 1999). The contribution of each reference site to the learning set and the inclusion criteria for topsoil samples were also modified, and ten Rock-Eval® parameters not considered in the first version of the model were proposed as potential predictor variables for this second version of the statistical model (see Sect. 2.2 and 2.4 and supplementary Table S1).

540

Using this improved design, all Rock-Eval® temperature parameters showed positive values of Spearman's rho coefficient with the proportion of the centennial stable SOC fraction in topsoils (Table 2), when a few of them showed counterintuitive significant negative correlations using the learning set of the first version of PARTY<sub>SOC</sub> (Cécillon et al., 2018). This confirms the generic link between SOC thermal stability and its *in situ* biogeochemical stability: centennially 545 stable SOC is thermally stable, even though thermostable SOC fractions are a mixture of centennially stable and active SOC (Fig. 1; Barré et al., 2016; Gregorich et al., 2015; Plante et al., 2013; Sanderman and Grandy, 2020; Schiedung et al., 2017). Some Rock-Eval® temperature parameters were within the five most important predictor variables for both PARTY<sub>SOCv2.0</sub> (T70<sub>CO2\_OX</sub>, T90<sub>HC\_PYR</sub>) and PARTY<sub>SOCv2.0\_EU</sub> (T50<sub>CO2\_PYR</sub>) statistical models (Table 2).

550 Contrary to the first version of the PARTY<sub>SOC</sub> statistical model, the second version tested several Rock-Eval® parameters directly linked to soil carbon content as potential predictor variables. TOC<sub>RE6</sub> was selected as a meaningful predictor variable for PARTY<sub>SOCv2.0</sub> and PARTY<sub>SOCv2.0\_EU</sub>. Its negative correlation with the centennial stable SOC proportion (Table 2) was



expected, according to the calculation of the latter (see Sect. 2.3). This is in line with results from SOC-dating techniques and with most multi-compartmental models of SOC dynamics suggesting that the proportion of the most persistent SOC 555 fraction is a decreasing function of total SOC (Huggins et al., 1998; Rühlmann, 1999). Indeed, the *ex-post* optimized initial value of the proportion of the inert SOC fraction for the simple AMG model of SOC dynamics is higher (0.60 on average) for SOC-poor temperate topsoils with a long-term arable history than for SOC-rich temperate topsoils with a long-term grassland history (0.47 on average; Clivot et al., 2019). Contrarily, the empirical function commonly used to initialize the size of the inert SOC fraction of the multi-compartmental RothC model predicts an increased proportion of inert SOC with 560 increased total SOC (Falloon et al., 1998). This empirical function needs to be examined upon these results.

Interestingly, S2 (pyrolysable volatile hydrocarbon effluents) and PC (total pyrolysable organic carbon), two other Rock-Eval® parameters linked to SOC content showed a stronger negative relationship than TOC<sub>RE6</sub> with the proportion of the 565 centennial stable SOC fraction. Both variables are within the three most important predictor variables for PARTY<sub>SOCv2.0</sub> and PARTY<sub>SOCv2.0\_EU</sub> while TOC<sub>RE6</sub> was ranked sixth or ninth out of the 18 predictor variables (Table 2). Other Rock-Eval® parameters related to the pyrolysable SOC fraction (PC/TOC<sub>RE6</sub> and HI, both negatively related to the centennial stable SOC proportion) were also important predictor variables for both models. The results suggest that a simple decreasing 570 function of total SOC content cannot accurately predict the centennial stable SOC proportion in topsoils, according to the recent report by Clivot et al. (2019). They also confirm the generic elemental stoichiometry of the centennial stable SOC fraction: it is consistently depleted in hydrogen (Barré et al., 2016; Gregorich et al., 2015; Poeplau et al., 2019); and they illustrate the usefulness of the pyrolysis step of Rock-Eval® thermal analysis and its volatile hydrocarbon effluents quantification to infer the proportion of the centennial stable SOC fraction in unknown topsoils.

#### 4.2 Capability of the second version of PARTY<sub>SOC</sub> to partition the centennial stable and active SOC fractions

The learning set of the second version of the PARTY<sub>SOC</sub> statistical model was significantly diversified compared with the 575 first version. Its reference topsoil samples now represent wider pedoclimatic conditions (supplementary Table S2), and it includes one long-term vegetation change site as reference site (La Cabaña). Reference topsoils from the Colombian site of La Cabaña fit well into the global learning set of the statistical model: they did not alter its overall performance. The root-mean-square errors of PARTY<sub>SOCv2.0</sub> (internal or random splitting validation procedures) are comparable to the ones of the model's first version, where the content of the centennial stable SOC fraction was inferred exclusively from plant-free soils 580 (Fig. 2a, Table 3; Cécillon et al., 2018). Similarly, the expansion of the reference learning topsoil sample set to new soil types (Acrisol at La Cabaña, Chernozem at Bad Lauchstädt; FAO, 2014), soil texture (loamy coarse sand at Askov; supplementary Table S2), soil pH (in H<sub>2</sub>O, with values as low as 4 at La Cabaña; supplementary Table S2) and climate (tropical at La Cabaña; supplementary Table S2) did not alter the performance of the model, when assessed using the internal or random splitting validation procedures (Fig. 2a, Table 3). Conversely, the leave-one-site-out validation procedure 585 illustrated that the second version of PARTY<sub>SOC</sub> is currently not capable of accurately partitioning SOC into its centennial



stable and active fractions in soil samples coming from pedoclimates that differ strongly from the ones included in the learning set (sites of La Cabaña and Bad Lauchstädt; Fig. 2b, Table 3b). This indicates that like all machine-learning approaches, the  $\text{PARTY}_{\text{SOC}}$  model gains progressively more genericity (*i.e.*, capability to fairly predict the centennially stable SOC proportion in unknown soils) as its learning set integrates soils from new pedoclimates. To this respect, the 590 second version of  $\text{PARTY}_{\text{SOC}}$  significantly extends the model's validity range to new pedoclimates (tropical Cambisols, continental Chernozems and temperate loamy coarse sand Luvisols). Contrarily, the relatively high prediction error of both  $\text{PARTY}_{\text{SOCv2.0}}$  and  $\text{PARTY}_{\text{SOCv2.0}_{\text{EU}}}$  models at Rothamsted (high  $\text{rRMSEP}$ ), a site with a pedoclimate rather similar to some of the other European sites included in the learning set of  $\text{PARTY}_{\text{SOC}}$ , may be due to an inaccurate estimate (overestimation) of the centennially stable SOC content at this site. Indeed, a report from an ancient LTBF trial at 595 Rothamsted (drain gauge experiment; Jenkinson and Coleman, 1994), on the same soil type than the Highfield bare fallow experiment, showed a measured total SOC content of  $7.9 \text{ g C kg}^{-1}$ , which is lower than our current estimate of the centennially stable SOC content ( $9.72 \text{ g C kg}^{-1}$ ; Table 1). Yet, the conditions of the drain gauge experiment, with a basic soil pH value of 7.9 due to heavy dressing of chalk on Rothamsted's arable lands before the 19<sup>th</sup> century (Avery and Catt, 1995; Jenkinson and Coleman, 1994), may not be directly comparable to the conditions of the Highfield bare fallow experiment 600 showing acidic pH values ranging from 5.2 to 6.3 (supplementary Table S2).

The predictive ability of the second version of  $\text{PARTY}_{\text{SOC}}$  was more thoroughly assessed compared to the first version of the statistical model. Specifically, the sensitivity of model performance to the reference sites included in the learning set demonstrates that local models —with learning sets composed of soils from pedoclimates similar to the ones of the soils 605 from the prediction set— showed better predictive ability of the centennially stable SOC proportion compared to a global statistical model (Fig. 3). While the current learning set is composed of too few reference sites to implement local modelling, this suggests that the European version  $\text{PARTY}_{\text{SOCv2.0}_{\text{EU}}}$  should be preferred to the global  $\text{PARTY}_{\text{SOCv2.0}}$  model when predicting the centennially stable SOC proportion in unknown soils from Europe. The mean prediction error of 0.15 obtained using the leave-one-site-out validation procedure of  $\text{PARTY}_{\text{SOCv2.0}_{\text{EU}}}$  (with a  $\text{rRMSEP}$  of 0.27; Table 3a) is probably a 610 conservative estimate of the accuracy of this model to partition the centennially stable and active SOC fractions over a wide pedoclimatic range of agricultural topsoils in Northwestern Europe.

#### 4.3 Future developments and recommended applications of the second version of the $\text{PARTY}_{\text{SOC}}$ model

The second version of the  $\text{PARTY}_{\text{SOC}}$  model is based on six long-term agricultural sites including an LTBF treatment located in Northwestern Europe and one vegetation change ( $\text{C}_4$  to  $\text{C}_3$  plants) site located in Colombia. The very first future 615 improvement for the machine-learning model is to pursue the expansion of the pedoclimatic diversity of its learning set. A few additional LTBF sites and several  $\text{C}_3$  to  $\text{C}_4$  plants (or  $\text{C}_4$  to  $\text{C}_3$ ) long-term vegetation change sites (including space-for-time substitution, like the site of La Cabaña) could be used to achieve this goal. A potential complement lies in a few long-term experimental sites with soil archives and treatments experiencing contrasting SOC stock changes. Radiocarbon



measurements on recent and archived soil samples from such sites can be used to infer the content of the centennially stable  
620 SOC fraction in topsoils (Hsieh, 1992), but also in subsoils, to allow extending the model to deeper soil horizons. Following  
the method developed by Buyanovsky and Wagner (1998b, 1998a) and Huggins et al. (1998), the content of the centennially  
stable SOC fraction can also be estimated at a few additional long-term experiments with contrasted SOC inputs. A  
promising complement to these strategies lies in numerous long-term sites where time series of SOC inputs, outputs and  
stocks are well constrained (*i.e.*, long-term experiments or long-term monitoring sites in various types of ecosystems  
625 including arable land, grassland and forest). It is possible to reliably infer the content of the centennially stable SOC fraction  
at these sites using simple models of SOC dynamics like AMG (Clivot et al., 2019). Combining all these strategies could  
help expanding significantly the learning set of  $\text{PARTY}_{\text{SOC}}$  to soil samples from diverse climates, ecosystems, soil types and  
soil depths. When the learning set of  $\text{PARTY}_{\text{SOC}}$  will integrate a sufficient diversity of soil samples, a second future  
improvement of the model lies in the comparison of different machine-learning algorithms as well as the testing of local  
630 modelling approaches, as commonly used in soil spectroscopy studies (Dangal et al., 2019; Gogé et al., 2012; Ramirez-  
Lopez et al., 2013b, 2013a).

Meanwhile, the current version of the  $\text{PARTY}_{\text{SOC}}$ v2.0 model and especially its European version  $\text{PARTY}_{\text{SOC}}\text{v2.0}_{\text{EU}}$  already  
provide accurate predictions of the size of the centennially stable and active SOC fraction in agricultural topsoils of a large  
635 diversity of pedoclimatic conditions (Fig. 2; Table 3). We consider that  $\text{PARTY}_{\text{SOC}}\text{v2.0}_{\text{EU}}$  is mature enough (see Sect. 3.3,  
3.4 and 4.2) to be reliably applied on agricultural topsoils in Northwestern Europe, or to be tested on topsoils of other  
ecosystems under similar pedoclimates for research purposes. The  $\text{PARTY}_{\text{SOC}}\text{v2.0}_{\text{EU}}$  model is available on public  
repositories as an R script and an R data file (see Sect. Data and code availability).  $\text{PARTY}_{\text{SOC}}\text{v2.0}_{\text{EU}}$  generates predictions  
of the centennially stable and active SOC proportions and contents (in  $\text{g C kg}^{-1}$ ; obtained by multiplying the centennially  
640 stable and active SOC proportions by  $\text{TOC}_{\text{RE6}}$ ) in unknown soil samples, using their measured Rock-Eval® parameters.

The second version of  $\text{PARTY}_{\text{SOC}}$  enables the reliable partitioning of SOC into its centennially stable and active SOC  
fractions (Fig. 2). The validation of the model at the scale of Northwestern Europe presented here ( $\text{PARTY}_{\text{SOC}}\text{v2.0}_{\text{EU}}$ )  
constitutes a breakthrough in the metrology of SOC kinetic pools. It represents a great improvement compared to other  
645 approaches that consistently fail to achieve a proper separation of active from stable SOC (Fig. 1; Hsieh, 1992; von Lützow  
et al., 2007). Those methods such as the physical or physico-chemical SOC fractionation schemes have been developed to  
initialize the size of SOC kinetic pools of models (Skjemstad et al., 2004; Zimmermann et al., 2007a) and some of them are  
now implemented on large topsoil sample sets at the national or continental scale in Europe (Cotrufo et al., 2019; Vos et al.,  
2018) and Australia (Gray et al., 2019; Viscarra Rossel et al., 2019). A similar implementation in soil monitoring networks  
650 of Rock-Eval® measurements combined with the second version of  $\text{PARTY}_{\text{SOC}}$  will provide a more accurate quantification  
of the functionally different SOC fractions that are centennially stable or active (Fig. 1). Large-scale Rock-Eval®  
measurements and the combined application of the  $\text{PARTY}_{\text{SOC}}\text{v2.0}_{\text{EU}}$  model are already ongoing in the French soil



monitoring network for soil quality assessment (RMQS; Jolivet et al., 2018). We recommend undertaking similar works in other national and international soil monitoring networks. The second version of  $\text{PARTY}_{\text{SOC}}$  can also be directly employed  
655 as a SOC pools partitioning method for simple models of SOC dynamics that are built on the same dualistic conceptual approach of SOC persistence (*i.e.*, active *vs.* inert SOC pools). The accuracy of these simple models, such as AMG, is highly sensitive to the proper partitioning of SOC kinetic pools (Clivot et al., 2019), and could thus strongly benefit from the second version of  $\text{PARTY}_{\text{SOC}}$ .

660 We envision a significant contribution of the  $\text{PARTY}_{\text{SOC}}$  machine-learning model based on Rock-Eval® thermal analysis to the forthcoming large-scale availability of accurate information on the size of the centennially stable or active SOC fractions. Such accurate information will foster (1) the initiatives of soil health assessment and monitoring and (2) the modelling works of SOC dynamics and of the climate regulation function of soils.

### Data and code availability

665 The Rock-Eval® data of the 105 reference topsoil samples of  $\text{PARTY}_{\text{SOCv2.0}}$  are provided in supplementary Table S3. The R script used to extract Rock-Eval® 6 raw data and calculate Rock-Eval® parameters; the Rock-Eval® data and the R script used to build  $\text{PARTY}_{\text{SOCv2.0}}$  and  $\text{PARTY}_{\text{SOCv2.0}_{\text{EU}}}$  models and test their performance; and the  $\text{PARTY}_{\text{SOCv2.0}_{\text{EU}}}$  model (available as an R script and an R data file) can be accessed on GitHub at <https://github.com/lauric-cecillon/PARTYsoc> and on Zenodo at the permanent link <https://doi.org/10.5281/zenodo.4446138>.

### 670 Acknowledgments

The French Agence nationale de la recherche (StoreSoilC project, grant ANR-17-CE32-0005), the French Agence de la transition écologique (ADEME), and Ville de Paris (SOCUTE project, emergence(s) program) funded this research. We are indebted to the generations of technicians and scientists that started and managed the long-term experiments and archives of soil samples used in this work. We thank Rothamsted Research for access to samples and data from the Rothamsted Sample  
675 Archive and the electronic Rothamsted Archive (e-RA). The Rothamsted Long-term Experiments are supported by the UK Biotechnology and Biological Sciences Research Council under the National Capabilities programme grant (BBS/E/C/000J0300), and by the Lawes Agricultural Trust. We thank David Montagne and Joël Michelin (AgroParisTech, France) who provided information on the soil characteristics at Grignon. We thank our colleagues of the Soil Science research group at Ecole normale supérieure (Paris, France), especially Samuel Abiven, Núria Catalán, Bertrand Guenet and  
680 Marcus Schiedung who provided advices that improved this manuscript.



## Author contributions

L.C. and P.B. designed the study with contributions from C.C. and F.B.. F.B. and F.S. performed the Rock-Eval® measurements. L.C. wrote the R scripts used to calculate Rock-Eval® parameters and built the second version of the PARTY<sub>SOC</sub> model with contributions from P.B., L.N.S. and E.K.. B.T.C., U.F., S.H., T.K., I.M., F.v.O, C.P., J.C.Q. provided 685 the topsoil samples and the metadata of the reference sites. L.C. and P.B. wrote the manuscript with contributions from all authors.

## Competing interests

The authors declare that they have no conflict of interest.

## References

690 695 700 Abiven, S., Menasseri, S. and Chenu, C.: The effects of organic inputs over time on soil aggregate stability – A literature analysis, *Soil Biology and Biochemistry*, 41(1), 1–12, <https://doi.org/10.1016/j.soilbio.2008.09.015>, 2009.  
Amundson, R., Berhe, A. A., Hopmans, J. W., Olson, C., Sztein, A. E. and Sparks, D. L.: Soil and human security in the 21st century, *Science*, 348(6235), 1261071–1261071, <https://doi.org/10.1126/science.1261071>, 2015.  
Ansorge, H.: Die Wirkung des Stallmistes im “Statischen Düngungsversuch” Lauchstädt, 2. Mitteilung: Veränderung des Humusgehaltes im Boden, *Albrecht-Thaer-Archiv*, 10(4), 401–412, 1966.  
Avery, B. W. and Catt, J. A.: The soil at Rothamsted, Lawes Agricultural Trust, Harpenden. <https://repository.rothamsted.ac.uk/item/87192>, 1995.  
Baldock, J. A., Hawke, B., Sanderman, J. and Macdonald, L. M.: Predicting contents of carbon and its component fractions in Australian soils from diffuse reflectance mid-infrared spectra, *Soil Res.*, 51(8), 577, <https://doi.org/10.1071/SR13077>, 2013.  
Balesdent, J.: The significance of organic separates to carbon dynamics and its modelling in some cultivated soils, *European Journal of Soil Science*, 47(4), 485–493, <https://doi.org/10.1111/j.1365-2389.1996.tb01848.x>, 1996.  
Balesdent, J. and Guillet, B.: Les datations par le <sup>14</sup>C des matières organiques des sols. Contribution à l'étude de l'humification et du renouvellement des substances humiques, *Science du sol*, 2, 93–112, 1982.  
705 Balesdent, J. and Mariotti, A.: Measurement of soil organic matter turnover using <sup>13</sup>C natural abundance, in *Mass spectrometry of soils*, edited by T. W. Boutton and S. I. Yamasaki, pp. 83–111, <https://www.researchgate.net/publication/257855705>, 1996.  
Balesdent, J., Mariotti, A. and Guillet, B.: Natural <sup>13</sup>C abundance as a tracer for studies of soil organic matter dynamics, *Soil Biology and Biochemistry*, 19(1), 25–30, [https://doi.org/10.1016/0038-0717\(87\)90120-9](https://doi.org/10.1016/0038-0717(87)90120-9), 1987.



710 Balesdent, J., Wagner, G. H. and Mariotti, A.: Soil organic matter turnover in long-term field experiments as revealed by carbon-13 natural abundance, *Soil Science Society of America Journal*, 52(1), 118–124, <https://doi.org/10.2136/sssaj1988.03615995005200010021x>, 1988.

Balesdent, J., Basile-Doelsch, I., Chadoeuf, J., Cornu, S., Derrien, D., Fekiacova, Z. and Hatté, C.: Atmosphere–soil carbon transfer as a function of soil depth, *Nature*, 559(7715), 599–602, <https://doi.org/10.1038/s41586-018-0328-3>, 2018.

715 Barré, P., Eglin, T., Christensen, B. T., Ciais, P., Houot, S., Kätterer, T., van Oort, F., Peylin, P., Poulton, P. R., Romanenkov, V. and Chenu, C.: Quantifying and isolating stable soil organic carbon using long-term bare fallow experiments, *Biogeosciences*, 7(11), 3839–3850, <https://doi.org/10.5194/bg-7-3839-2010>, 2010.

Barré, P., Plante, A. F., Cécillon, L., Lutfalla, S., Baudin, F., Bernard, S., Christensen, B. T., Eglin, T., Fernandez, J. M., Houot, S., Kätterer, T., Le Guillou, C., Macdonald, A., van Oort, F. and Chenu, C.: The energetic and chemical signatures of 720 persistent soil organic matter, *Biogeochemistry*, 130(1–2), 1–12, <https://doi.org/10.1007/s10533-016-0246-0>, 2016.

Behar, F., Beaumont, V. and De B. Penteado, H. L.: Rock-Eval 6 Technology: Performances and Developments, *Oil & Gas Science and Technology - Rev. IFP*, 56(2), 111–134, <https://doi.org/10.2516/ogst:2001013>, 2001.

Beleites, C. and Sergo, V.: hyperSpec: a package to handle hyperspectral data sets in R. <https://github.com/cbeleites/hyperSpec>, 2020.

725 Bellon-Maurel, V., Fernandez-Ahumada, E., Palagos, B., Roger, J.-M. and McBratney, A.: Critical review of chemometric indicators commonly used for assessing the quality of the prediction of soil attributes by NIR spectroscopy, *TrAC Trends in Analytical Chemistry*, 29(9), 1073–1081, <https://doi.org/10.1016/j.trac.2010.05.006>, 2010.

Borchers, H. W.: pracma: practical numerical math functions. <https://CRAN.R-project.org/package=pracma>, 2019.

Breiman, L.: Random Forests, *Machine Learning*, 45(1), 5–32, <https://doi.org/10.1023/A:1010933404324>, 2001.

730 Buyanovsky, G. A. and Wagner, G. H.: Carbon cycling in cultivated land and its global significance, *Global Change Biology*, 4(2), 131–141, <https://doi.org/10.1046/j.1365-2486.1998.00130.x>, 1998a.

Buyanovsky, G. A. and Wagner, G. H.: Changing role of cultivated land in the global carbon cycle, *Biology and Fertility of Soils*, 27(3), 242–245, <https://doi.org/10.1007/s003740050427>, 1998b.

Canty, A. and Ripley, B.: boot: bootstrap R (S-Plus) functions., 2020.

735 Cardinael, R., Eglin, T., Guenet, B., Neill, C., Houot, S. and Chenu, C.: Is priming effect a significant process for long-term SOC dynamics? Analysis of a 52-years old experiment, *Biogeochemistry*, 123(1–2), 203–219, <https://doi.org/10.1007/s10533-014-0063-2>, 2015.

Cécillon, L., Cassagne, N., Czarnes, S., Gros, R. and Brun, J.-J.: Variable selection in near infrared spectra for the biological characterization of soil and earthworm casts, *Soil Biology and Biochemistry*, 40(7), 1975–1979, 740 <https://doi.org/10.1016/j.soilbio.2008.03.016>, 2008.

Cécillon, L., Baudin, F., Chenu, C., Houot, S., Jolivet, R., Kätterer, T., Lutfalla, S., Macdonald, A., van Oort, F., Plante, A. F., Savignac, F., Soucémarijanadin, L. N. and Barré, P.: A model based on Rock-Eval thermal analysis to quantify the size of



the centennially persistent organic carbon pool in temperate soils, *Biogeosciences*, 15(9), 2835–2849, <https://doi.org/10.5194/bg-15-2835-2018>, 2018.

745 Cerri, C., Feller, C., Balesdent, J., Victoria, R. and Plenccassagne, A.: Application du traçage isotopique naturel en  $^{13}\text{C}$ , à l'étude de la dynamique de la matière organique dans les sols, *Comptes Rendus de l'Académie des sciences*, 423–428, 1985.

Christensen, B. T. and Johnston, A. E.: Soil organic matter and soil quality—Lessons learned from long-term experiments at Askov and Rothamsted, in *Developments in Soil Science*, vol. 25, pp. 399–430, Elsevier, [https://doi.org/10.1016/S0166-2481\(97\)80045-1](https://doi.org/10.1016/S0166-2481(97)80045-1), 1997.

750 Christensen, B. T., Thomsen, I. K. and Eriksen, J.: The Askov long-term experiments: 1894–2019: a unique research platform turns 125 years, DCA - Nationalt Center for Fødevarer og Jordbrug, Tjele. <https://dcapub.au.dk/djfpublikation/djfpdf/DCArapport151.pdf>, 2019.

Clivot, H., Mouny, J.-C., Duparque, A., Dinh, J.-L., Denoroy, P., Houot, S., Vertès, F., Trochard, R., Bouthier, A., Sagot, S. and Mary, B.: Modeling soil organic carbon evolution in long-term arable experiments with AMG model, *Environmental Modelling & Software*, 118, 99–113, <https://doi.org/10.1016/j.envsoft.2019.04.004>, 2019.

755 Cotrufo, M. F., Ranalli, M. G., Haddix, M. L., Six, J. and Lugato, E.: Soil carbon storage informed by particulate and mineral-associated organic matter, *Nat. Geosci.*, 12(12), 989–994, <https://doi.org/10.1038/s41561-019-0484-6>, 2019.

Coulston, J. W., Blinn, C. E., Thomas, V. A. and Wynne, R. H.: Approximating prediction uncertainty for random forest regression models, *Photogram Engng Rem Sens*, 82(3), 189–197, <https://doi.org/10.14358/PERS.82.3.189>, 2016.

760 Dangal, S., Sanderman, J., Wills, S. and Ramirez-Lopez, L.: Accurate and precise prediction of soil properties from a large mid-infrared spectral library, *Soil Syst.*, 3(1), 11, <https://doi.org/10.3390/soilsystems3010011>, 2019.

Davison, A. C. and Hinkley, D. V.: *Bootstrap methods and their application*, Cambridge University Press, Cambridge ; New York, NY, USA., 1997.

Disnar, J. R., Guillet, B., Keravis, D., Di-Giovanni, C. and Sebag, D.: Soil organic matter (SOM) characterization by Rock-765 Eval pyrolysis: scope and limitations, *Organic Geochemistry*, 34(3), 327–343, [https://doi.org/10.1016/S0146-6380\(02\)00239-5](https://doi.org/10.1016/S0146-6380(02)00239-5), 2003.

Falloon, P., Smith, P., Coleman, K. and Marshall, S.: Estimating the size of the inert organic matter pool from total soil organic carbon content for use in the Rothamsted carbon model, *Soil Biology and Biochemistry*, 30(8–9), 1207–1211, [https://doi.org/10.1016/S0038-0717\(97\)00256-3](https://doi.org/10.1016/S0038-0717(97)00256-3), 1998.

770 Falloon, P. D. and Smith, P.: Modelling refractory soil organic matter, *Biology and Fertility of Soils*, 30(5–6), 388–398, <https://doi.org/10.1007/s003740050019>, 2000.

FAO: *World reference base for soil resources 2014: international soil classification system for naming soils and creating legends for soil maps.*, FAO, Rome., 2014.

Franko, U. and Merbach, I.: Modelling soil organic matter dynamics on a bare fallow Chernozem soil in Central Germany, 775 *Geoderma*, 303, 93–98, <https://doi.org/10.1016/j.geoderma.2017.05.013>, 2017.

Genuer, R. and Poggi, J.-M.: *Random Forests with R*, Springer International Publishing, Cham., 2020.



Gogé, F., Joffre, R., Jolivet, C., Ross, I. and Ranjard, L.: Optimization criteria in sample selection step of local regression for quantitative analysis of large soil NIRS database, *Chemometrics and Intelligent Laboratory Systems*, 110(1), 168–176, <https://doi.org/10.1016/j.chemolab.2011.11.003>, 2012.

780 Gray, J., Karunaratne, S., Bishop, T., Wilson, B. and Veeragathipillai, M.: Driving factors of soil organic carbon fractions over New South Wales, Australia, *Geoderma*, 353, 213–226, <https://doi.org/10.1016/j.geoderma.2019.06.032>, 2019.

Gregorich, E. G., Gillespie, A. W., Beare, M. H., Curtin, D., Sanei, H. and Yanni, S. F.: Evaluating biodegradability of soil organic matter by its thermal stability and chemical composition, *Soil Biology and Biochemistry*, 91, 182–191, <https://doi.org/10.1016/j.soilbio.2015.08.032>, 2015.

785 He, Y., Trumbore, S. E., Torn, M. S., Harden, J. W., Vaughn, L. J. S., Allison, S. D. and Randerson, J. T.: Radiocarbon constraints imply reduced carbon uptake by soils during the 21st century, *Science*, 353(6306), 1419–1424, <https://doi.org/10.1126/science.aad4273>, 2016.

Hénin, S. and Dupuis, M.: Bilan de la matière organique des sols, *Annales Agronomiques*, 1, 17–29, 1945.

790 Hénin, S. and Turc, L.: Essai de fractionnement des matières organiques du sol, *Comptes rendus de l'Académie d'agriculture de France*, 35, 41–43, 1949.

Houot, S., Molina, J. A. E., Chaussod, R. and Clapp, C. E.: Simulation by NCSOIL of net mineralization in soils from the Deherain and 36 parcelles fields at Grignon, *Soil Science Society of America Journal*, 53(2), 451–455, <https://doi.org/10.2136/sssaj1989.03615995005300020023x>, 1989.

795 Hsieh, Y.-P.: Pool size and mean age of stable soil organic carbon in croplands, *Soil Science Society of America Journal*, 56(2), 460–464, <https://doi.org/10.2136/sssaj1992.03615995005600020049x>, 1992.

Huggins, D. R., Buyanovsky, G. A., Wagner, G. H., Brown, J. R., Darmody, R. G., Peck, T. R., Lesoing, G. W., Vanotti, M. B. and Bundy, L. G.: Soil organic C in the tallgrass prairie-derived region of the corn belt: effects of long-term crop management, *Soil and Tillage Research*, 47(3–4), 219–234, [https://doi.org/10.1016/S0167-1987\(98\)00108-1](https://doi.org/10.1016/S0167-1987(98)00108-1), 1998.

800 IPBES: Summary for policymakers of the assessment report on land degradation and restoration of the Intergovernmental Science-Policy Platform on Biodiversity and Ecosystem Services, edited by R. J. Scholes, L. Montanarella, E. Brainich, E. Brainich, N. Barger, B. ten Brink, M. Cantele, B. Erasmus, J. Fisher, T. Gardner, T. G. Holland, F. Kohler, S. Kotiaho, G. von Maltitz, G. Nangendo, R. Pandit, J. Parrotta, M. D. Potts, S. Prince, M. Sankaran, and L. Willemen, Intergovernmental Science-Policy Platform on Biodiversity and Ecosystem Services., 2018.

IPCC: Climate change and land: an IPCC special report on climate change, desertification, land degradation, sustainable land management, food security, and greenhouse gas fluxes in terrestrial ecosystems, Intergovernmental Panel on Climate Change., 2019.

ISO 10694: Soil quality — Determination of organic and total carbon after dry combustion (elementary analysis). <https://www.iso.org/standard/18782.html>, 1995.



Jaconi, A., Poeplau, C., Ramirez-Lopez, L., Van Wesemael, B. and Don, A.: Log-ratio transformation is the key to  
810 determining soil organic carbon fractions with near-infrared spectroscopy, *Eur J Soil Sci*, 70(1), 127–139,  
<https://doi.org/10.1111/ejss.12761>, 2019.

Janzen, H. H.: The soil carbon dilemma: shall we hoard it or use it?, *Soil Biology and Biochemistry*, 38(3), 419–424,  
<https://doi.org/10.1016/j.soilbio.2005.10.008>, 2006.

Jenkinson, D. S.: The turnover of organic carbon and nitrogen in soil, *Phil. Trans. R. Soc. Lond. B*, 329(1255), 361–368,  
815 <https://doi.org/10.1098/rstb.1990.0177>, 1990.

Jenkinson, D. S. and Coleman, K.: Calculating the annual input of organic matter to soil from measurements of total organic  
carbon and radiocarbon, *Eur J Soil Science*, 45(2), 167–174, <https://doi.org/10.1111/j.1365-2389.1994.tb00498.x>, 1994.

Jenkinson, D. S., Adams, D. E. and Wild, A.: Model estimates of CO<sub>2</sub> emissions from soil in response to global warming,  
*Nature*, 351(6324), 304–306, <https://doi.org/10.1038/351304a0>, 1991.

820 Johnston, A. E., Poulton, P. R. and Coleman, K.: Soil organic matter: its importance in sustainable agriculture and carbon  
dioxide fluxes, in *Advances in Agronomy*, vol. 101, pp. 1–57, Elsevier, [https://doi.org/10.1016/S0065-2113\(08\)00801-8](https://doi.org/10.1016/S0065-2113(08)00801-8), ,  
2009.

Jolivet, C., Almeida-Falcon, J. L., Berché, P., Boulonne, L., Fontaine, M., Gouny, L., Lehmann, S., Maître, B., Ratié, C.,  
Schellenberger, E. and Soler-Dominguez, N.: Manuel du Réseau de mesures de la qualité des sols. RMQS2 : deuxième  
825 campagne métropolitaine, 2016 – 2027, Version 3, INRA, US 1106 InfoSol, Orléans, France., 2018.

Kätterer, T., Bolinder, M. A., Andrén, O., Kirchmann, H. and Menichetti, L.: Roots contribute more to refractory soil  
organic matter than above-ground crop residues, as revealed by a long-term field experiment, *Agriculture, Ecosystems &*  
*Environment*, 141(1–2), 184–192, <https://doi.org/10.1016/j.agee.2011.02.029>, 2011.

Keesstra, S. D., Bouma, J., Wallinga, J., Tittonell, P., Smith, P., Cerdà, A., Montanarella, L., Quinton, J. N., Pachepsky, Y.,  
830 van der Putten, W. H., Bardgett, R. D., Moolenaar, S., Mol, G., Jansen, B. and Fresco, L. O.: The significance of soils and  
soil science towards realization of the United Nations Sustainable Development Goals, *SOIL*, 2(2), 111–128,  
<https://doi.org/10.5194/soil-2-111-2016>, 2016.

Khedim, N., Cécillon, L., Poulenard, J., Barré, P., Baudin, F., Marta, S., Rabatel, A., Dentant, C., Cauvy-Fraunié, S.,  
Anthelme, F., Gielly, L., Ambrosini, R., Franzetti, A., Azzoni, R. S., Caccianiga, M. S., Compostella, C., Clague, J.,  
835 Tielidze, L., Messager, E., Choler, P. and Ficetola, G. F.: Topsoil organic matter build-up in glacier forelands around the  
world, *Glob Change Biol*, gcb.15496, <https://doi.org/10.1111/gcb.15496>, 2020.

Koch, A., McBratney, A., Adams, M., Field, D., Hill, R., Crawford, J., Minasny, B., Lal, R., Abbott, L., O'Donnell, A.,  
Angers, D., Baldock, J., Barbier, E., Binkley, D., Parton, W., Wall, D. H., Bird, M., Bouma, J., Chenu, C., Flora, C. B.,  
Goulding, K., Grunwald, S., Hempel, J., Jastrow, J., Lehmann, J., Lorenz, K., Morgan, C. L., Rice, C. W., Whitehead, D.,  
840 Young, I. and Zimmermann, M.: Soil security: solving the global soil crisis, *Glob Policy*, 4(4), 434–441,  
<https://doi.org/10.1111/1758-5899.12096>, 2013.



Körschens, M., Weigel, A. and Schulz, E.: Turnover of soil organic matter (SOM) and long-term balances - tools for evaluating sustainable productivity of soils, *Z. Pflanzenernaehr. Bodenk.*, 161(4), 409–424, <https://doi.org/10.1002/jpln.1998.3581610409>, 1998.

845 Lal, R.: Soil carbon sequestration impacts on global climate change and food security, *Science*, 304(5677), 1623–1627, <https://doi.org/10.1126/science.1097396>, 2004.

Lavalée, J. M., Soong, J. L. and Cotrufo, M. F.: Conceptualizing soil organic matter into particulate and mineral-associated forms to address global change in the 21st century, *Glob Change Biol.*, 26(1), 261–273, <https://doi.org/10.1111/gcb.14859>, 2020.

850 Liaw, A. and Wiener, M.: Classification and regression by randomForest, *R News*, 2(3), 18–22, 2002.

Ludwig, B., Schulz, E., Rethemeyer, J., Merbach, I. and Flessa, H.: Predictive modelling of C dynamics in the long-term fertilization experiment at Bad Lauchstädt with the Rothamsted Carbon Model, *European Journal of Soil Science*, 58(5), 1155–1163, <https://doi.org/10.1111/j.1365-2389.2007.00907.x>, 2007.

855 Luo, Y., Ahlström, A., Allison, S. D., Batjes, N. H., Brovkin, V., Carvalhais, N., Chappell, A., Ciais, P., Davidson, E. A., Finzi, A., Georgiou, K., Guenet, B., Hararuk, O., Harden, J. W., He, Y., Hopkins, F., Jiang, L., Koven, C., Jackson, R. B., Jones, C. D., Lara, M. J., Liang, J., McGuire, A. D., Parton, W., Peng, C., Randerson, J. T., Salazar, A., Sierra, C. A., Smith, M. J., Tian, H., Todd-Brown, K. E. O., Torn, M., van Groenigen, K. J., Wang, Y. P., West, T. O., Wei, Y., Wieder, W. R., Xia, J., Xu, X., Xu, X. and Zhou, T.: Toward more realistic projections of soil carbon dynamics by Earth system models, *Global Biogeochem. Cycles*, 30(1), 40–56, <https://doi.org/10.1002/2015GB005239>, 2016.

860 von Lützow, M., Kögel-Knabner, I., Ekschmitt, K., Flessa, H., Guggenberger, G., Matzner, E. and Marschner, B.: SOM fractionation methods: Relevance to functional pools and to stabilization mechanisms, *Soil Biology and Biochemistry*, 39(9), 2183–2207, <https://doi.org/10.1016/j.soilbio.2007.03.007>, 2007.

Monnier, G., Turc, C. and Jeanson Luusinang, C.: Une methode de fractionnement densimetrique par centrifugation des matieres organiques du sol, *Annales Agronomiques*, 13(1), 55–63, 1962.

865 Nikiforoff, C. C.: Some General Aspects of the Chernozem Formation, *Soil Science Society of America Journal*, 1(C), 333–342, <https://doi.org/10.2136/sssaj1937.03615995000100000060x>, 1936.

van Oort, F., Paradelo, R., Proix, N., Delarue, G., Baize, D. and Monna, F.: Centennial fertilization-induced soil processes control trace metal dynamics. Lessons from a long-term bare fallow experiment, *Soil Syst.*, 2(2), 23, <https://doi.org/10.3390/soilsystems2020023>, 2018.

870 Patil, A., Huard, D. and Fonnesbeck, C.: PyMC: Bayesian stochastic modelling in Python, *J. Stat. Soft.*, 35(4), <https://doi.org/10.18637/jss.v035.i04>, 2010.

Pellerin, S., Bamière, L., Launay, C., Martin, R., Schiavo, M., Angers, D., Augusto, L., Balesdent, J., Basile-Doelsch, I., Bellassen, V., Cardinael, R., Cécillon, L., Ceschia, E., Chenu, C., Constantin, J., Darroussin, J., Delacote, P., Delame, N., Gastal, F., Gilbert, D., Graux, A.-I., Guenet, B., Houot, S., Klumpp, K., Letort, E., Litrico, I., Martin, M., Menasseri-Aubry, S., Meziere, D., Morvan, T., Mosnier, C., Roger-Estrade, J., Saint-André, L., Sierra, J., Therond, O., Viaud, V., Grateau, R.,



Le Perche, S., Savini, I. and Rechauchère, O.: Stocker du carbone dans les sols français, quel potentiel au regard de l'objectif 4 pour 1000 et à quel coût ?, Agence de l'Environnement et de la Maîtrise de l'Energie (ADEME) et le Ministère de l'Agriculture et de l'Alimentation (MAA), INRA. <https://hal.archives-ouvertes.fr/hal-02284521>, last access: 23 May 2020, 2019.

880 Petersen, B. M., Berntsen, J., Hansen, S. and Jensen, L. S.: CN-SIM—a model for the turnover of soil organic matter. I. Long-term carbon and radiocarbon development, *Soil Biology and Biochemistry*, 37(2), 359–374, <https://doi.org/10.1016/j.soilbio.2004.08.006>, 2005.

Plante, A. F., Beaupré, S. R., Roberts, M. L. and Baisden, T.: Distribution of radiocarbon ages in soil organic matter by thermal fractionation, *Radiocarbon*, 55(2), 1077–1083, <https://doi.org/10.1017/S0033822200058215>, 2013.

885 Poeplau, C., Don, A., Dondini, M., Leifeld, J., Nemo, R., Schumacher, J., Senapati, N. and Wiesmeier, M.: Reproducibility of a soil organic carbon fractionation method to derive RothC carbon pools: Soil carbon fractionation ring trial, *Eur J Soil Sci*, 64(6), 735–746, <https://doi.org/10.1111/ejss.12088>, 2013.

Poeplau, C., Don, A., Six, J., Kaiser, M., Benbi, D., Chenu, C., Cotrufo, M. F., Derrien, D., Gioacchini, P., Grand, S., Gregorich, E., Griepentrog, M., Gunina, A., Haddix, M., Kuzyakov, Y., Kühnel, A., Macdonald, L. M., Soong, J., Trigalet, S., Vermeire, M.-L., Rovira, P., van Wesemael, B., Wiesmeier, M., Yeasmin, S., Yevdokimov, I. and Nieder, R.: Isolating organic carbon fractions with varying turnover rates in temperate agricultural soils – A comprehensive method comparison, *Soil Biology and Biochemistry*, 125, 10–26, <https://doi.org/10.1016/j.soilbio.2018.06.025>, 2018.

890 Poeplau, C., Barré, P., Cécillon, L., Baudin, F. and Sigurdsson, B. D.: Changes in the Rock-Eval signature of soil organic carbon upon extreme soil warming and chemical oxidation - A comparison, *Geoderma*, 337, 181–190, <https://doi.org/10.1016/j.geoderma.2018.09.025>, 2019.

Quezada, J. C., Etter, A., Ghazoul, J., Buttler, A. and Guillaume, T.: Carbon neutral expansion of oil palm plantations in the Neotropics, *Sci. Adv.*, 5(11), eaaw4418, <https://doi.org/10.1126/sciadv.aaw4418>, 2019.

R Core Team: R: a language and environment for statistical computing, R Foundation for Statistical Computing, Vienna, Austria. <https://www.R-project.org/>, 2020.

900 Ramirez-Lopez, L., Behrens, T., Schmidt, K., Rossel, R. A. V., Dematté, J. A. M. and Scholten, T.: Distance and similarity-search metrics for use with soil vis–NIR spectra, *Geoderma*, 199, 43–53, <https://doi.org/10.1016/j.geoderma.2012.08.035>, 2013a.

Ramirez-Lopez, L., Behrens, T., Schmidt, K., Stevens, A., Dematté, J. A. M. and Scholten, T.: The spectrum-based learner: A new local approach for modeling soil vis–NIR spectra of complex datasets, *Geoderma*, 195–196, 268–279, 905 <https://doi.org/10.1016/j.geoderma.2012.12.014>, 2013b.

RStudio Team: RStudio: integrated development for R, RStudio, Inc., Boston, MA. <http://www.rstudio.com/>, 2020.

Rühlmann, J.: A new approach to estimating the pool of stable organic matter in soil using data from long-term field experiments, *Plant and Soil*, 213(1/2), 149–160, <https://doi.org/10.1023/A:1004552016182>, 1999.



910 Saenger, A., Cécillon, L., Sebag, D. and Brun, J.-J.: Soil organic carbon quantity, chemistry and thermal stability in a mountainous landscape: A Rock-Eval pyrolysis survey, *Organic Geochemistry*, 54, 101–114, https://doi.org/10.1016/j.orggeochem.2012.10.008, 2013.

915 Saenger, A., Cécillon, L., Poulenard, J., Bureau, F., De Daniéli, S., Gonzalez, J.-M. and Brun, J.-J.: Surveying the carbon pools of mountain soils: A comparison of physical fractionation and Rock-Eval pyrolysis, *Geoderma*, 241–242, 279–288, https://doi.org/10.1016/j.geoderma.2014.12.001, 2015.

920 Sanderman, J. and Grandy, A. S.: Ramped thermal analysis for isolating biologically meaningful soil organic matter fractions with distinct residence times, *SOIL*, 6(1), 131–144, https://doi.org/10.5194/soil-6-131-2020, 2020.

Sanderman, J., Hengl, T. and Fiske, G. J.: Soil carbon debt of 12,000 years of human land use, *Proc Natl Acad Sci USA*, 114(36), 9575–9580, https://doi.org/10.1073/pnas.1706103114, 2017.

925 Schiedung, M., Don, A., Wordell-Dietrich, P., Alcántara, V., Kuner, P. and Guggenberger, G.: Thermal oxidation does not fractionate soil organic carbon with differing biological stabilities, *J. Plant Nutr. Soil Sci.*, 180(1), 18–26, https://doi.org/10.1002/jpln.201600172, 2017.

Schulte, R. P. O., Creamer, R. E., Donnellan, T., Farrelly, N., Fealy, R., O'Donoghue, C. and O'hUallachain, D.: Functional land management: A framework for managing soil-based ecosystem services for the sustainable intensification of agriculture, *Environmental Science & Policy*, 38, 45–58, https://doi.org/10.1016/j.envsci.2013.10.002, 2014.

925 Sebag, D., Verrecchia, E. P., Cécillon, L., Adatte, T., Albrecht, R., Aubert, M., Bureau, F., Cailleau, G., Copard, Y., Decaens, T., Disnar, J.-R., Hetényi, M., Nyilas, T. and Trombino, L.: Dynamics of soil organic matter based on new Rock-Eval indices, *Geoderma*, 284, 185–203, https://doi.org/10.1016/j.geoderma.2016.08.025, 2016.

930 Shi, Z., Allison, S. D., He, Y., Levine, P. A., Hoyt, A. M., Beem-Miller, J., Zhu, Q., Wieder, W. R., Trumbore, S. and Randerson, J. T.: The age distribution of global soil carbon inferred from radiocarbon measurements, *Nat. Geosci.*, https://doi.org/10.1038/s41561-020-0596-z, 2020.

Skjemstad, J. O., Spounger, L. R., Cowie, B. and Swift, R. S.: Calibration of the Rothamsted organic carbon turnover model (RothC ver. 26.3), using measurable soil organic carbon pools, *Soil Res.*, 42(1), 79, https://doi.org/10.1071/SR03013, 2004.

935 Soucémariandin, L., Cécillon, L., Chenu, C., Baudin, F., Nicolas, M., Girardin, C. and Barré, P.: Is Rock-Eval 6 thermal analysis a good indicator of soil organic carbon lability? – A method-comparison study in forest soils, *Soil Biology and Biochemistry*, 117, 108–116, https://doi.org/10.1016/j.soilbio.2017.10.025, 2018a.

Soucémariandin, L. N., Cécillon, L., Guenet, B., Chenu, C., Baudin, F., Nicolas, M., Girardin, C. and Barré, P.: Environmental factors controlling soil organic carbon stability in French forest soils, *Plant Soil*, 426(1–2), 267–286, https://doi.org/10.1007/s11104-018-3613-x, 2018b.

940 Stoorvogel, J. J., Bakkenes, M., Brink, B. J. E. and Temme, A. J. A. M.: To what extent did we change our soils? A global comparison of natural and current conditions, *Land Degrad. Develop.*, 28(7), 1982–1991, https://doi.org/10.1002/ldr.2721, 2017.



Strobl, C., Malley, J. and Tutz, G.: An introduction to recursive partitioning: Rationale, application, and characteristics of classification and regression trees, bagging, and random forests., *Psychological Methods*, 14(4), 323–348, <https://doi.org/10.1037/a0016973>, 2009.

945 Taghizadeh-Toosi, A., Cong, W.-F., Eriksen, J., Mayer, J., Olesen, J. E., Keel, S. G., Glendining, M., Kätterer, T. and Christensen, B. T.: Visiting dark sides of model simulation of carbon stocks in European temperate agricultural soils: allometric function and model initialization, *Plant Soil*, 450(1–2), 255–272, <https://doi.org/10.1007/s11104-020-04500-9>, 2020.

Trumbore, S. E., Vogel, J. S. and Southon, J. R.: AMS 14C measurements of fractionated soil organic matter: an approach to 950 deciphering the soil carbon cycle, *Radiocarbon*, 31(03), 644–654, <https://doi.org/10.1017/S0033822200012248>, 1989.

Viscarra Rossel, R. A. and Hicks, W. S.: Soil organic carbon and its fractions estimated by visible-near infrared transfer functions: Vis-NIR estimates of organic carbon and its fractions, *Eur J Soil Sci*, 66(3), 438–450, <https://doi.org/10.1111/ejss.12237>, 2015.

Viscarra Rossel, R. A., Lee, J., Behrens, T., Luo, Z., Baldock, J. and Richards, A.: Continental-scale soil carbon composition 955 and vulnerability modulated by regional environmental controls, *Nat. Geosci.*, 12(7), 547–552, <https://doi.org/10.1038/s41561-019-0373-z>, 2019.

Vos, C., Jaconi, A., Jacobs, A. and Don, A.: Hot regions of labile and stable soil organic carbon in Germany – Spatial variability and driving factors, *SOIL*, 4(2), 153–167, <https://doi.org/10.5194/soil-4-153-2018>, 2018.

Wehrens, R.: *Chemometrics with R: Multivariate Data Analysis in the Natural and Life Sciences*, Springer Berlin 960 Heidelberg, Berlin, Heidelberg., 2020.

Wickham, H.: *stringr: simple, consistent wrappers for common string operations.* <https://CRAN.R-project.org/package=stringr>, 2019.

Wiesmeier, M., Urbanski, L., Hobley, E., Lang, B., von Lützow, M., Marin-Spiotta, E., van Wesemael, B., Rabot, E., Ließ, M., Garcia-Franco, N., Wollschläger, U., Vogel, H.-J. and Kögel-Knabner, I.: Soil organic carbon storage as a key function 965 of soils - A review of drivers and indicators at various scales, *Geoderma*, 333, 149–162, <https://doi.org/10.1016/j.geoderma.2018.07.026>, 2019.

Zimmermann, M., Leifeld, J., Schmidt, M. W. I., Smith, P. and Fuhrer, J.: Measured soil organic matter fractions can be related to pools in the RothC model, *Eur J Soil Science*, 58(3), 658–667, <https://doi.org/10.1111/j.1365-2389.2006.00855.x>, 2007a.

970 Zimmermann, M., Leifeld, J. and Fuhrer, J.: Quantifying soil organic carbon fractions by infrared-spectroscopy, *Soil Biology and Biochemistry*, 39(1), 224–231, <https://doi.org/10.1016/j.soilbio.2006.07.010>, 2007b.